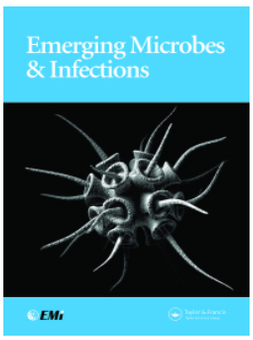

Emerging Microbes & Infections

ISSN: (Print) (Online) Journal homepage: https://www.tandfonline.com/loi/temi20

N-chlorotaurine is highly active against respiratory viruses including SARS-CoV-2 (COVID-19) in vitro

Michaela Lackner, Annika Rössler, André Volland, Marlena Nastassja Stadtmüller, Brigitte Müllauer, Zoltan Banki, Johannes Ströhle, Angela Luttick, Jennifer Fenner, Bettina Sarg, Leopold Kremser, Paul Tone, Heribert Stoiber, Dorothee von Laer, Thorsten Wolff, Carsten Schwarz & Markus Nagl

To cite this article: Michaela Lackner, Annika Rössler, André Volland, Marlena Nastassja Stadtmüller, Brigitte Müllauer, Zoltan Banki, Johannes Ströhle, Angela Luttick, Jennifer Fenner, Bettina Sarg, Leopold Kremser, Paul Tone, Heribert Stoiber, Dorothee von Laer, Thorsten Wolff, Carsten Schwarz & Markus Nagl (2022): N-chlorotaurine is highly active against respiratory viruses including SARS-CoV-2 (COVID-19) in vitro, Emerging Microbes & Infections, DOI: 10.1080/22221751.2022.2065932

To link to this article: https://doi.org/10.1080/22221751.2022.2065932

Publisher: Taylor & Francis & The Author(s). Published by Informa UK Limited, trading as Taylor & Francis Group, on behalf of Shanghai Shangyixun Cultural Communication Co., Ltd

Journal: *Emerging Microbes & Infections*

DOI: 10.1080/22221751.2022.2065932

N-chlorotaurine is highly active against respiratory viruses including SARS-CoV-2 (COVID-19) in vitro

Michaela Lackner[a], Annika Rössler[b], André Volland[b], Marlena Nastassja Stadtmüller[c,d], Brigitte Müllauer[b], Zoltan Banki[b], Johannes Ströhle[a], Angela Luttick[e], Jennifer Fenner[e], Bettina Sarg[f], Leopold Kremser[f], Paul Tone[g], Heribert Stoiber[b], Dorothee von Laer[b], Thorsten Wolff[c], Carsten Schwarz[h], Markus Nagl[a]*

[a]Institute of Hygiene and Medical Microbiology, Medical University of Innsbruck, Innsbruck, Austria;

[b]Institute of Virology, Medical University of Innsbruck, Innsbruck, Austria;

[c]Unit 17-Influenza and Other Respiratory Viruses, Robert Koch-Institute, Berlin, Germany;

[d]Current address: Institute of Medical Microbiology and Virology, Universitätsklinikum Carl Gustav Carus, Dresden, Germany;

[e]360biolabs Pty Ltd, Melbourne, Australia;

[f]Institute of Medical Biochemistry, Biocenter, Medical University of Innsbruck, Innsbruck, Austria;

[g]Innovative Biomedical Concepts, Inc., Staten Island, New York;

[h]CF Center Westbrandenburg, Division Cystic Fibrosis, Pediatric Clinic Westbrandenburg, Potsdam, Germany

Co-senior-authors DvL, TW, CS, MN

*Corresponding author: Markus Nagl, Assoc.Prof., MD, Institute of Hygiene and Medical Microbiology, Medical University of Innsbruck, Schöpfstr. 41 A-6020 Innsbruck / Austria, Tel. +43-(0)512-9003-70708, Fax +43-(0)512-9003-73700, E-mail: m.nagl@i-med.ac.at
ORCID: 0000-0002-1225-9349

Abstract

N-chlorotaurine (NCT) a long-lived oxidant generated by leukocytes, can be synthesized chemically and applied topically as an anti-infective to different body sites, including the lung via inhalation. Here, we demonstrate the activity of NCT against viruses causing acute respiratory tract infections, namely severe acute respiratory syndrome coronavirus 2 (SARS-CoV-2), influenza viruses, and respiratory syncytial virus (RSV).

Virucidal activity of NCT was tested in plaque assays, confirmed by RT-qPCR assays. Attack on virus proteins was investigated by mass spectrometry.

NCT revealed broad virucidal activity against all viruses tested at 37°C and pH 7. A significant reduction in infectious particles of SARS-CoV-2 isolates from early 2020 by 1 $\log_{10}$ was detected after 15 min of incubation in 1% NCT. Proteinaceous material simulating body fluids enhanced this activity by transchlorination mechanisms (1 -2 $\log_{10}$ reduction within 1 – 10 minutes). Tested SARS-CoV-2 variants B.1.1.7 (Alpha) und B.1.351 (Beta) showed a similar susceptibility. Influenza virus infectious particles were reduced by 3 $\log_{10}$ (H3N2) to 5 $\log_{10}$ (H1N1pdm), RSV by 4 $\log_{10}$. Mass spectrometry of NCT-treated SARS-CoV-2 spike protein and 3C-like protease, influenza virus hemagglutinin and neuraminidase,

and RSV fusion glycoprotein disclosed multiple sites of chlorination and oxidation as the molecular mechanism of action.

Application of 1.0% NCT as a prophylactic and therapeutic strategy against acute viral respiratory tract infections deserves comprehensive clinical investigation.

Keywords: N-chlorotaurine, COVID-19, influenza, respiratory syncytial virus, antiviral, anti-infective, antiseptic, respiratory tract

Main Text

Introduction

The coronavirus disease 2019 (COVID-19) pandemic has been the major challenge for human health in this 21st century. Nearly two years into the pandemic, no highly effective treatment with small molecules is established so far, while sufficient vaccinations were more rapidly developed. Application of *N*-chlorotaurine (Cl-NH-CH_2-CH_2-SO_3Na, NCT), a safe, well tolerated, endogenous, mild antiseptic with anti-inflammatory properties may be a significant step forward to combat COVID-19 and other viral respiratory tract infections. NCT as an inhaled anti-infective has already demonstrated broad-spectrum microbicidal activity against bacteria, fungi, viruses and protozoa. Here, we aimed to establish the virucidal activity of NCT against three main viruses responsible for lower respiratory tract infections, namely severe acute respiratory syndrome coronavirus 2 (SARS-CoV-2), influenza A virus, and respiratory syncytial viruses (RSV).

The COVID-19 pandemic is caused by SARS-CoV-2. The pandemic is affecting individuals, populations, and health systems far beyond infection. The virus might persist globally and become a prolonged or permanent threat [1,2]. Up to date, there has been a breakthrough regarding vaccination, and a majority of the available vaccines are effective

against the currently circulating virus variants of SARS-CoV-2. However, this may be changed with future mutations, and a highly sufficient and well tolerated medication for therapy and prophylaxis will be important particularly until the respective sufficient vaccines will have been developed. The race for a cure is a global effort and different approaches have been proposed and are currently studied [1,3]. Another major public concern is posed by influenza viruses, which annually cause 3 – 5 million cases of severe illness and about 290 000 to 650 000 of death worldwide [4]. Protection by the yearly influenza virus vaccine is unsatisfactory and resistance against existing antiviral drugs develops rapidly [5]. Therefore, new tools to combat influenza viruses are urgently needed.

One less known intervention is inhalation therapy with antiviral agents. An appeal for the inhaled route of administration has been published recently [6]. A first advantage is direct delivery of a high concentration of the medication to the lung, where the virus causes most of the severe problems [7]. Furthermore, topically applied therapies that are not systemically distributed avoid interactions with systemic medications, which are frequently necessary in elderly or multimorbid patients who are particularly at risk for severe COVID-19 complications [8]. An ideal inhaled drug should have broad-spectrum antimicrobial activity to cover not only SARS-CoV-2, but also co-infections and superinfections with other respiratory viruses and microorganisms (bacteria and fungi) [9-11]. Antiviral drugs are often specific to distinct viruses, but identifying the virus causing an infection requires logistic and diagnostic efforts, which in the case of SARS-CoV-2 amounts to at best one to two days for a diagnosis[12]. Such an ideal inhaled broad-spectrum drug mentioned above could be applied instantly regardless of the pathogen causing the respiratory illness and would thus eliminate the need for time-consuming diagnostics. Another key requirement is anti-inflammatory activity of the compound to downregulate the “cytokine storm”, particularly for SARS-CoV-2, which causes hyper-inflammation in severe cases [13].

One molecule that fulfils the criteria of broad-spectrum antimicrobial (virucidal, bactericidal, fungicidal, protozoocidal) and anti-inflammatory activity [14,15], and good tolerability upon inhalation is *N*-chlorotaurine (Cl-NH-CH_2-CH_2-SO_3^-) [16]. It is known since the 1970's as a product of activated human granulocytes and monocytes and belongs to the long-lived oxidants and chloramines formed by the myeloperoxidase via hypochlorous acid to combat invading pathogens [17-19] (Fig. 1). Moreover, *N*-chlorotaurine is thought to be involved in the control of inflammation by downregulating of nuclear factor kappaB activation, chemokines and proinflammatory cytokines such as tumor necrosis factor alpha, some prostaglandins and interleukins like IL-6 [15,20,21]. The synthesis of the sodium salt of *N*-chlorotaurine (Cl-NH-CH_2-CH_2-SO_3Na, NCT) was successful in our laboratory [22], which enabled its development as an endogenous anti-infective and mild antiseptic in human medicine. As an active chlorine compound belonging to the class of chloramines, it has the typical broad-spectrum microbicidal activity without development of resistance against Gram-positive and Gram-negative bacteria including multi-resistant strains, yeasts and moulds, protozoa, and worm larvae (for review see [14,23,24]). Broad-spectrum activity was found against adenoviruses [25-27], herpes viruses 1 and 2 [26,27], human immunodeficiency virus [28], and it was shown *in vivo* against adeno and herpes viruses in epidemic keratoconjunctivitis up to a phase II study as well as in herpes zoster in a case report, respectively [29-31]. Activity against coxsackievirus A24 and enterovirus 70 was found by the NCT-derivative *N*,*N*-dichloro-dimethyltaurine *in vitro* [32].

Over the last years, inhalation of NCT has been investigated and developed in detail. Enhanced bactericidal and fungicidal activity has been found in the presence of lung epithelial cells [33]. Tolerability of repeatedly inhaled NCT has been confirmed in the normal lung and in a streptoccoccal inflammation model each in pigs, and in the normal lung of mice [34-36]. In humans, tolerability was confirmed in a placebo-controlled phase I clinical study [16]. Only minor and transient adverse effects were found, i.e. chlorine taste and occasional tickle

in the throat [16]. NCT is not distributed systemically, which explains the absence of systemic adverse effects.

A safe, well tolerated, endogenous, inhaled substance with broad-spectrum activity against pathogens supported by anti-inflammatory properties may be a significant step forward for treatment of COVID-19 and other viral infections of the lower airways without the need of further diagnostics to discriminate between the infectious agents. In this regard, the aim of the present study was to establish and characterize the virucidal activity of NCT against three major viruses responsible for respiratory infections in humans, namely SARS-CoV-2, influenza viruses, and RSV *in vitro*.

Materials and methods

Reagents

N-chlorotaurine sodium salt (NCT, molecular weight 181.57 g/l, lot 2020-03-17) was prepared in pharmaceutical quality as established at our Department and frozen at minus 20°C for storage [22]. For testing, it was freshly dissolved in phosphate-buffered saline (PBS) at pH 7.1 (7.0 – 7.2) to desired stock concentrations between 1.0% (55.08 mM) and 10%.
As inactivation solution for NCT, a mixture of 1.0% methionine and 1.0% histidine (met/his, L-methionine and L-histidine, both from Carl Roth GmbH, Karlsruhe, Germany) in distilled water was used [37]. For tests in peptone, peptone enzymatic digest from Casein was applied (Fluka no. 82303, Sigma-Aldrich GmbH, Buchs, Switzerland). RPMI-1640 medium and fetal calf serum (FCS) were from Sigma-Aldrich GmbH, too.

Viruses, virus cell culture and preparation of viral suspensions

SARS-CoV-2

Robert Koch-Institute, Berlin (RKI).

SARS-CoV-2 BavPat1 strain was obtained from Christian Drosten's laboratory at the Institute of Virology at Charité Universitätsmedizin Berlin. Vero E6 cells were maintained in DMEM (supplemented with 10% FCS, 2 mM L-glutamine, non-essential amino acids, 1mM sodium pyruvate, 100 mg/ml streptomycin and 100 units/ml penicillin). For virus stock preparation, Vero E6 monolayer cultures grown in 75 cm^2 cell culture flasks were infected with a multiplicity of infection (MOI) of 0.01 in PBS (supplemented with 0.3% BA) for 2 days at 37°C and 5.0% CO_2. The supernatant was harvested and stored at minus 80°C until use.

Biolabs, Melbourne (Biolabs).

COVID-19 strain used was SARS-CoV-2 hCoV-19/Australia/VIC01/2020 (Melbourne's Peter Doherty Institute for Infection and Immunity, Melbourne, Australia). Parent stock of the virus was passaged twice in Vero cells. A working stock was generated at 360biolabs by two further passages in Vero cells in virus growth media, which comprised Minimal Essential Medium without L-glutamine supplemented with 1.0% (w/v) L-glutamine 1.0 µg/ml of TPCK-Trypsin, 0.2% BSA, 1 x Pen/Strep, and 1.0% Insulin Transferrin Selenium (ITS), then a further 2 passages in Vero E6 cells in growth media. This growth media comprised MEM supplemented with 1.0% (w/v) L-glutamine, 4.0 µg/ml of TPCK-Trypsin and 2.0% (v/v) heat inactivated FBS.

African Green Monkey Kidney (Vero E6) cells (ATCC-CRL1586) were sub-cultured to generate cell bank stocks in cell growth medium, which comprised Minimal Essential Medium without L-glutamine supplemented with 10% (v/v) heat-inactivated Fetal Bovine Serum and 1.0% (w/v) L-glutamine. Cell stocks were frozen at minus 80°C overnight and then transferred to liquid nitrogen. Vero E6 cells were passaged for a maximum of 13

passages, after which a new working cell bank stock was retrieved from liquid nitrogen for further use. Vero E6 cells were seeded into 96-well plates at 2 x 10^4 cells / well in 100 µl E6 seeding media (Minimal Essential Medium supplemented with 1.0% (w/v) L-glutamine, 2.0% FBS). Plates were incubated overnight at 37°C, 5.0% CO_2.

Institute of Virology, Innsbruck.

SARS-CoV-2 wildtype isolate 1.2 was a clinical isolate from a patients' respiratory swab sample in Innsbruck, Austria from March 2020. The SARS-CoV-2 Alpha (B.1.1.7, Isolate C63.1, EPI_ISL_3277382) and Beta (B.1.351, Isolate C24.1, EPI_ISL_1123262) variants originated from such swab samples, too. Virus stocks were produced on Vero/TMPRSS2 cells, kindly provided by Dr. Markus Hoffmann and Prof. Stefan Pöhlmann, Leibniz Institute for Primate Research, Göttingen, Germany [38]. Cells were cultured in DMEM plus 10% FCS and Pen/Strep. For Virus stock production, 80% confluent Vero/TMPRSS2 cells were infected with a MOI of 0.01 in DMEM plus 2.0% FCS. The supernatant was harvested 60 h post infection. Virus aliquots were stored at minus 80°C.

Influenza

Robert Koch-Institute, Berlin (RKI).

Influenza A/Panama/2007/1999 (H3N2) virus was grown in the allantois cavity of 11 day old embryonated chicken eggs for 2 days. Virus was harvested, clarified by centrifugation (300xg, 10 min) and stored at minus 80°C until use. Madin-Darby-Canine-Kidney (MDCK) II cells (ATCC) were maintained in MEM (supplemented with 10% FCS, 2 mM L-glutamine, 100 mg/ml streptomycin and 100 units/ml penicillin) at 37°C and 5.0% CO2.

Institute of Hygiene and Medical Microbiology, Innsbruck.

Influenza A/Singapore/Hongkong/2339/2000 (H1N1) was kindly provided by H. Katinger, Institute of Applied Microbiology, University of Natural Resources and Applied Life Sciences, Vienna, Austria. Influenza A/Swine Origin Virus (S-OIV)/California/2009 (H1N1pdm) was a clinical isolate from Innsbruck, Austria.

Influenza viruses were grown on MDCK cells (Collection of Cell Lines in Veterinary Medicine, Friedrich-Loeffler-Institut, Federal Research Institute for Animal Health, Greifswald, Germany). MDCK cells were grown in 25 cm^2 cell culture flasks (Sarstedt, Inc. Newton, NC, USA) in RPMI plus 10% FCS to a monolayer. The medium was replaced by 5 ml RPMI without FCS, and 10 µl of 1 mg/ml trypsin (final concentration 0.002 mg/ml) was added to activate neuraminidase. Viral suspension deep frozen at minus 80°C in RPMI (200 µl) was added. After 60 h of incubation at 37°C, a cytopathic effect was seen in all cells, and the supernatant was taken and centrifuged at 275 × g. The supernatant again was used as viral suspension for the tests.

RSV

RSV long strain, (kindly provided by T. Grunwald, Fraunhofer Institute for Cell Therapy and Immunology, Leipzig, Germany), was generated by infection of HEp2 cells at low MOI as described previously [39]. Virus titers were determined in plaque assays by infection of HEp2 with serial dilutions of the virus followed by immunocytochemical staining with polyclonal goat antibody against RSV (Gt X RSV, Merck) and HRP-conjugated rabbit polyclonal anti-goat IgG (Novusbio). 3-Amino-9-ethylcarbazole (AEC, Sigma) was used as a chromogen in immunohistochemistry to visualize the RSV infected cells.

Virus inactivation tests (quantitative killing assays) with NCT

General overview of the test method

The viral suspension was mixed with NCT (final concentration 0.1% to 1.0%) and incubated at 37°C for 1, 5, 7, 10, 15, 20, 30, 45, and 60 min. At the end of each incubation time, aliquots were removed and diluted in 1.0% met/his to inactivate NCT and to warrant exact incubation times. Virus inactivation was assessed by subsequent plaque assay, immunostaining or RT-qPCR as detailed below.

Controls were done in PBS or PBS with 5.0% peptone without NCT in parallel as well as inactivation controls. For the latter, 1.0% NCT was mixed with met/his before the addition of the respective virus. The virus must survive in the inactivation solution to obtain reliable results, which was the case in all tests.

SARS-CoV-2

Virus inactivation assay with plaque assay readout (RKI Berlin).

Three µl of concentrated virus suspension (4.76×10^9 PFU/ml) were added to 400 µl of NCT (1.0% or 0.1% in PBS), NCT with peptone (1.0% NCT, 5.0% peptone in PBS) or PBS and incubated at 37°C. After 5, 15, 30 and 60 min, 100 µl were removed and added to 100 µl of met/his. As inactivation control, 100 µl of 1.0% NCT or 1.0% NCT with 5.0% peptone were added to 100 µl of met/his and thereafter 0.75 µl of virus suspension were added. Infectious virus particles in all suspensions were determined with plaque assay. Briefly, a serial tenfold dilution of the virus suspension in PBS with 0.3% bovine albumin was added to confluent Vero E6 cells in 12-well plates, which were washed with PBS immediately before. After incubation at 37°C for 1h, the inoculum was removed followed by a washing step with PBS. Avicel-overlay medium (double-strength DMEM supplemented with 10% FCS, 1.0% DEAE dextran, 5.0% sodium bicarbonate and 1.25% Avicel) was added and plates incubated at 37°C

and 5.0% CO_2 for 3 days before staining with crystal violet for visualization of plaques. Counted plaques are expressed as plaque forming units per ml (PFU/ml).

Virus inactivation assay with plaque assay readout (GLP lab 360 biolabs, Melbourne). Cell seeding media were removed from a pre-seeded plate (assay plate) and cell monolayers were washed with PBS twice. A volume of 50 µl of non-supplemented MEM was added to all wells except the isopropanol positive control wells. A volume of 50 µl of (4.0% or 0.4%) NCT was added to NCT-treated wells, 50 µl of non-supplemented MEM was added to virus only wells and 100 µl of isopropanol (≥ 99.5%, Sigma-Aldrich) added to positive control wells. A 100 µl volume of SARS-CoV-2 (B3) that had been pre-diluted 1:10 in non-supplemented MEM was added to all wells. Plates were incubated for 5, 10, 20, and 60 min at 37°C, 5.0% CO_2. An additional 100 µl of virus growth media containing TPCK trypsin required for virus growth (MEM supplemented with 1.0% (w/v) L-glutamine, 2.0% FBS and 8 µg/ml TPCK trypsin) was added to plates pre-seeded with Vero E6 cells that samples were to be titrated onto.

At each time point, 100 µl of either 1.0% or 0.1% NCT media was removed from the assay plate and added to either 100 µl of met/his in distilled water to inactivate the NCT. The positive control and virus only controls were also diluted 1:2 into distilled water. Each sample was diluted a further 1:10 into virus growth media, MEM supplemented with 1.0% (w/v) L-glutamine and 2.0% FBS containing 4.0 µg/ml of TPCK trypsin (i.e. 100 µl of inactivated sample + 900 µl of virus growth media). The remaining virus after NCT inactivation was quantified by addition of 100 µl volume of 1:10 diluted inactivated NCT to triplicate wells of 96-well plate pre-seeded with Vero E6 cells. Plates were incubated at 37°C, 5.0% CO_2 for 4 days. Virus-induced CPE was scored visually. The $TCID_{50}$ of the virus suspension was determined using the method of Reed-Muench [40]. The virucidal effect was quantified as the

log_{10} reduction in virus titre compared to the SARS-CoV-2 control. Isopropanol (≥ 99.5%) was used as the assay positive control.

For inactivation controls, 100 µl of NCT at 4.0% and 0.4% was added to 100 µl of 4.0% met/his or 0.4% met/his prior to addition of virus. A volume of 100 µl of this inactivation mix was added to wash pre-seeded Vero E6 cells. To this, 100 µl of virus pre-diluted 1:10 in non-supplemented MEM was added and incubated at 37°C, 5.0% CO_2 for 10 min or 60 minutes. Following the incubations, 100 µl was diluted into 900 µl of virus growth media containing 4 µg/ml of TPCK trypsin (1:10). The remaining virus was quantified as outlined above.

Absence of cytotoxicity of inactivated NCT to the inoculated cell culture.

As a cytotoxicity control, the 1.0% NCT and 0.1% NCT was set up the same and inactivated by met/his as outlined above but instead of 100 µl of virus being added, 100 µl of non-supplemented MEM was added. These samples were treated exactly the same as above and titrated across pre-seeded cells to ascertain any cytotoxicity observed by the NCT. For cell viability staining, a 100 µl volume of a 3 mg/ml solution of 3-(4,5-dimethylthiazole-2-yl)-2,5-diphenyl tetrazolium bromide (MTT) was added to cytotoxicity control plates and incubated for 2 h at 37°C in a 5.0% CO_2 incubator. Wells were aspirated to dryness using a multichannel manifold attached to a vacuum chamber and formazan crystals solubilized by the addition of 200 µl 100% 2-Propanol at room temperature for 30 minutes. Absorbance was measured at 540 – 650 nm on a plate reader. Absorbance values were averaged and reported as % reduction of MTT to formazan.

Virus inactivation assay with immunostaining and RT-qPCR (Virology Innsbruck).

Each 150 µl of NCT (2.0% in PBS) and of virus suspension (in DMEM plus 2.0% FCS plus 2 mM glutamine, plus Pen/Strep) were mixed and incubated at 37°C. After each incubation

time, 50 µl were removed and transferred to an equal volume of met/his. Controls were done in PBS without NCT. As inactivation controls, 75 µl of 2.0% NCT in PBS were added to 150 µl of met/his, followed by addition of 75 µl virus suspension. After serial tenfold dilution of this suspension, 50 µl each were added to 90% confluent Vero/TMPRSS2 or Vero/TMPRSS2/ACE2 cells in 96-well plates, from which the medium was removed immediately before. After incubation of 1 h at 37°C, the supernatant was removed, and after a washing step with 100 µl of medium, 100 µl of fresh medium was added. After further 9 h incubation, cells were fixed for immunostaining or total RNA was extracted for RT-qPCR as described below.

Immunostaining (detection by antibodies and peroxidase-marked second antibody).
After fixation for 5 min with 96% EtOH, cells were blocked for 15 min with PBS containing 0.1% FCS. Subsequently, cells were stained using serum from a SARS-CoV-2 recovered patient and horse radish peroxidase (HRPO)-conjugated anti-human secondary antibody. The signal was developed using a 3-amino-9-ethylcarbazole (AEC) substrate. Infected cells were visible as red spots and the number of infected cells was counted using an ImmunoSpot S6 Ultra-V reader and CTL analyser *BioSpot*® 5.0 software (CTL Europe GmbH, Bonn, Germany).

RT-qPCR.
For RNA extraction, the supernatant was removed, and the cell monolayer was washed twice with PBS. The cells were lysed 5 min at room-temperature using 100 µl in-house direct lysis buffer (10 mM Tris-HCL pH 7.4, 25 nM NaCl, 0.5% IGEPAL, 10 Units RiboLock RNase Inhibitor in DEPC-treated water) [41]. Subsequently, 5 µl RNA was used in a one-step RT-qPCR assay using the iTaq^{TM} RT-PCR (BIO-RAD) kit and previously published primers and

probes specific for detection of the SARS-CoV-2 E Gene on a CFX96^{TM} real-time system (BIO-RAD) [42].

Virus titration by $TCID_{50}$.

Virus titrations were performed by tenfold serial dilution and end-point titration on 10^4 Vero/TMPRSS2/ACE2 cells per well in 96-well microtitre plates. Four days after inoculation, the CPE was analysed and the $TCID_{50}$ titre was calculated.

Influenza

Virus inactivation assay with plaque assay readout (RKI).

Eight µl of virus suspension (A/Panama/2007/1999 (H3N2), 1.3×10^8 PFU/ml) were added to 400 µl of NCT (1.0% or 0.1% in PBS) or PBS and incubated at 37°C. After 5, 15, 30 and 60 min, 100 µl were removed and added to 100 µl of met/his. As inactivation control, 100 µl of 1.0% NCT were added to 100 µl of met/his and thereafter 2 µl of virus suspension were added. Infectious virus particles in all suspensions were determined with plaque assay. Briefly, a serial tenfold dilution of the virus suspension in PBS with 0.3% bovine albumin was added to confluent MDCK II cells in 12-well plates, which were washed with PBS immediately before. After incubation at 37°C for 1 h, the inoculum was removed followed by a washing step with PBS. Avicel-overlay medium (double-strength MEM supplemented with 0.2% BA, 1.0% DEAE dextran, 5.0% sodium bicarbonate, 1 mg/ml TPCK-trypsin and 1.25% Avicel) was added and plates incubated at 37°C and 5.0% CO_2 for 2 days before staining with crystal violet for visualization of plaques. Counted plaques are expressed as plaque forming units per ml (PFU/ml).

Virus inactivation assay with plaque assay readout (Hygiene and Medical Microbiology Innsbruck).

MDCK cells (2 x 10^4 / well) were grown in 96- well flat microtitre plates (Becton Dickinson Labware and Company, Franklin Lakes, NJ USA) for 24 h in RPMI plus 10% FCS. Subsequently, the medium was replaced by 100 µl of plain RPMI per well.

Each viral strain (H1N1 and H1N1pdm) was tested separately. Tenfold concentrated NCT (10.0%, 5.0%, and 1.0%, respectively) in distilled water (50 µl; water without NCT for controls) was added to 450 µl of virus suspension in RPMI (pH 7.2) to a final concentration of 1.0%, 0.5%, and 0.1%, respectively, and incubated for 1, 5, and 10 min at 22°C. A separate series of experiments was done with a final concentration of 0.1% NCT (5.5 mM) plus 0.1% ammonium chloride (18.7 mM) (Merck) and 1 min incubation time. At the end of the incubation time, aliquots of 100 µl were removed and mixed with 100 µl of met/his to inactivate NCT. Aliquots of 11 µl of this viral suspension in inactivated NCT were added to the MDCK cells in 96-well microtitre plates containing 100 µl RPMI per well. A series of tenfold dilutions in microtitre plates was performed. Inoculated plates were incubated at 37°C and 5.0% CO_2 and evaluated for plaques after 5 days. As inactivation controls, 100 µl each of 1.0% NCT and met/his were mixed. An aliquot of 50 µl was added to 450 µl of virus suspension.

RSV

RSV was incubated in the presence or absence of NCT at a final concentration of 0.1% and 1.0% for 5, 10, 15, 30 and 60 minutes at 37°C. Virus (24 µl in DMEM plus 1.0% FCS and 2 mM L-glutamine) was mixed with 24 µl of NCT in PBS. Additional tests with higher organic load were done, where 24 µl of virus suspension was mixed with 12 µl of 10% or 1% peptone, followed by 12 µl of 4% or 0.4% NCT (final concentration 1% and 0.1% NCT).

After indicated time-points, 48 µl of met/his was added to stop the reaction. As inactivation control, NCT was preincubated with equal amount of met/his for 10 minutes at RT prior to incubation with RSV. Infectious virus particles in all samples were titrated in plaque assay using HEp2 cells as described above. Aliquots of 25 µl were serially diluted in 100 µl of medium (DMEM plus 10% FCS and 2 mM L-glutamine) in microtitre plates, and 100 µl of Hep2 cells were added.

Structural changes of viral proteins by NCT evaluated by mass spectrometry

Proteins of SARS-CoV-2, influenza virus and RSV essential for attachment and virus replication were chosen as examples for oxidative attack by NCT.

Full length spike protein of SARS-CoV-2 as purified recombinant protein expressed in HEK 293 cells, produced by EMD Millipore Corporation, Temecula, CA and delivered in Tris buffer, was purchased from Sigma-Aldrich (Cat. # AGX819, Lot # 3678862, molecular weight 138 kDa). The protein (100 µg), delivered in 125 µl buffer, was diluted with 75 µl water for injection (Fresenius Kabi Austria GmbH, Graz, Austria) to 0.5 µg/µl. Of this stock solution, 20 µl containing 10 µg of protein were mixed and incubated with 20 µl of 2% NCT in water for injection at 37°C for 30 min. For control, protein incubated in water alone was used. Samples were frozen at minus 20°C for storage before mass spectrometry.

Full length 3C-like proteinase (M^{pro}) of SARS-CoV-2 was purchased from Sigma-Aldrich (Cat. # SAE0172-200µg, Lot # 0000102583). The protein (200 µg), supplied lyophilized from 20 mM HEPES (pH 7.3), 2.5% Trehalose, and 0.05% Tween 20, was diluted with 200 µl water for injection (Fresenius Kabi Austria GmbH, Graz, Austria) to 1.0 µg/µl. Of this stock solution, 20 µl containing 20 µg of protein were mixed and incubated with 20 µl of 2% NCT in water for injection at 37°C for 30 min. For control, protein incubated in water alone was used. Samples were frozen at minus 20°C for storage before mass spectrometry.

Hemagglutinin from influenza H1N1 (A/Ohio/UR06-0091/2007, Cat. # 11687-V08H, Lot # LC15JU1007), neuraminidase from influenza H1N1 (A/California/04/2009, Cat. # 11058-V08B, Lot # LC13OC1108), and fusion glycoprotein of RSV (RSV-F, strain RSS-2, Cat. # 40037-V08B, Lot # LC10NO1507), all full length and supplied lyophilized were purchased from Sino Biological Europe GmbH (Eschborn, Germany). Hemagglutinin and neuraminidase were dissolved in 400 µl of water for injection (10 µg / 40 µl), fusion glycoprotein in 670 µl of 20mM Tris and 500mM NaCl (pH 7.5) (10 µg / 67 µl). To 40 µl of hemagglutinin and neuraminidase, 40 µl of 2% NCT, and to 67 µl of fusion glycoprotein, 67 µl of 2% NCT were added and incubated at 37°C for 30 min. Samples were frozen at minus 20°C for storage before mass spectrometry.

NCT and Tris-HCl buffer were removed using a 10 kDa molecular mass cut-off filter, Amicon® Ultra-0.5 Centrifugal Filter Device (Merck, Darmstadt, Germany). Samples, dissolved in 80 µl 100 mM NH4HCO3 (pH 8.0), were reduced with dithiothreitol 30 min at 56°C, alkylated with iodoacetamide 20 min at room temperature, and digested with trypsin (Promega, Madison, WI, USA) 6 h at 37°C. Digested samples were analyzed using an UltiMate 3000 RSCLnano-HPLC system coupled to a Q Exactive HF mass spectrometer (Thermo Scientific, Bremen, Germany) equipped with a Nanospray Flex ionization source. The peptides were separated on a homemade frit-less fused-silica micro-capillary column (75 µm i.d. x 280 µm o.d. x 17 cm length) packed with 2.4 µm reversed-phase C18 material (Reprosil). Solvents for HPLC were 0.1% formic acid (solvent A) and 0.1% formic acid in 85% acetonitrile (solvent B). The gradient profile was as follows: 0 - 4 min, 4% B; 4 - 34 min, 4 - 35% B; 34 - 39 min, 35 - 100% B, and 39 - 44 min, 100% B. The flow rate was 250 nl/min.

Database search was performed using Proteome Discoverer 2.2 (Thermo Scientific) with search engine Sequest and a database consisting of 210 proteins to which the sequence of the SARS-CoV-2 spike protein was added. Precursor and fragment mass tolerance was set to 10

ppm and 0.02 Da, respectively, and up to two missed cleavages were allowed. Variable modifications were oxidation and di-oxidation at Cys and Met, tri-oxidation at Cys, and chlorination at Phe, His, Trp and Tyr. Peptide identifications were filtered at 1% false discovery rate.

Statistics

Results are presented of mean values and standard deviation (SD) of generally at least three independent experiments each. Detection limits are indicated by dotted lines in the figures. Student's unpaired t-test, in cases of two groups, and one-way analysis of variance (ANOVA) and Dunnett's multiple-comparison test, in cases of more than two groups, were used to test for differences between the test and control groups. P values of < 0.05 were considered significant for all tests and indicated as * $p < 0.05$, ** $p < 0.01$, *** $p < 0.001$, **** $p < 0.0001$. Calculations were performed with GraphPad Prism 7.00 software (Graph- Pad, Inc., La Jolla, CA, USA).

Results

NCT was incubated with SARS-CoV-2, influenza A virus or RSV, followed by assessment of virus inactivation using various readouts. NCT at a clinically relevant concentration of 0.1% - 1.0% demonstrated virucidal activity against SARS-CoV-2 (SARS-CoV-2 BavPat1, hCoV-19/Australia/VIC01/2020, clinical isolate 1.2 Innsbruck from early 2020, as well as the B.1.1.7 (Alpha) und B.1.351 (Beta) variants of concern, influenza A virus, and RSV (RSV long strain). Longer NCT-exposure periods were required to inactivate SARS-CoV-2 than to

inactivate influenza viruses or RSV. In the presence of organic matter, inactivation of viruses was even enhanced so that a significant reduction of plaque forming units and infected cells, respectively, could be observed already after 5 min with SARS-CoV-2 by 1.0% NCT. Controls without NCT and specific inactivation controls showed full viral replication in all cases to warrant valid results. The typical multiplicity of target sites for NCT, which excludes the acquisition of distinct resistance mutations, was exemplarily demonstrated by mass spectrometry analysis of NCT-treated spike protein of SARS-CoV-2. Detailed results are presented in the following paragraphs.

Virucidal activity of NCT against SARS-CoV-2

Inactivation of SARS-CoV-2 wild type isolates from early 2020 was assessed by incubating stock virus with NCT for indicated time periods at 37°C and then determining the remaining infectious particles using plaque assay or immunostaining as well as determining virus inactivation via RT-qPCR or TCID50. Exact incubation times of virus with NCT were ensured by adding met/his at the end of the incubation period, which inactivates NCT. All assays demonstrated a significant inactivation of SARS-CoV-2 with slight differences according to the individual test method and strain used.

With plaque assay readout, a significant reduction in infectious particles was detected after 15 min of incubation, when incubating SARS-CoV-2 with NCT in a buffered aqueous solution (Fig. 2a). The mild oxidizing activity of the test antiseptic may explain why it took as long as 15 min to reduce infectious particles. In the presence of Vero cells (Fig. 2b) or particularly 5.0% peptone (Fig. 2a), however, a significant reduction of infectious virus particles occurred already after 5 min of incubation with 1.0% NCT. This remarkable enhancement of activity by organic load is typical for NCT and shown for viruses for the first time here and is explained most likely by transhalogenation (see discussion).

Virus inactivation assays with immunostaining readout showed a 50% reduction of infected cells after 1 min (not significant, $p = 0.085$), 20 – 80% reduction after 5 min ($p = 0.0102$), 81 – 91% after 7 min ($p < 0.01$), 81 – 97% after 10 min, 96 – 99% after 20 min, and > 99% after 30 min ($p < 0.0001$ for these values). A logarithmic scale with respective statistics is provided in Fig. 2c. The results found by RT-qPCR assay were similar with a highly significant reduction of genome copies (Fig. 2d). This was further confirmed by the TCID50 readout (Fig. 2e).

The representative isolates of SARS-CoV-2 variants of concern B.1.1.7 and B.1.351 tested in the virus inactivation assay with immunostaining showed the same susceptibility to NCT than wild type isolates (Fig. 2f and 2g). For the B.1.1.7 variant, the reduction of infected cells was 42 - 54% after 1 min ($p = 0.0109$), 50 – 71% after 5 min ($p < 0.01$), 62 – 99% after 10 min ($p < 0.01$), 99 – 100% after 20 min ($p < 0.001$), and 100% after 30 min ($p < 0.001$). The values for the B.1.351 variant were 0 - 48% after 1 min (not significant, $p = 0.313$), 54 – 72% after 5 min ($p < 0.01$), 82 – 97% after 10 min ($p < 0.001$), 99 – 100% after 20 min ($p < 0.001$), and 100% after 30 min ($p < 0.001$).

The antiviral activity was concentration-dependent. Inactivation controls demonstrated full inactivation of 1.0% NCT by 1.0% methionine / 1.0% histidine (met/his). This was valid for all tests and viruses in this study. Absence of cytotoxicity of inactivated NCT to the inoculated cell culture was proved by MTT testing with values of MTT reduction of 94.1 ± 8.5 (0.1% NCT plus 0.1% met/his) and 100.3 ± 5.6 (PBS control) ($p = 0.12$ by Student's unpaired t-test).

Virucidal activity of NCT against influenza viruses

Inactivation of influenza viruses was assessed like inactivation of SARS-CoV-2 by incubating stock virus with NCT for indicated time periods at 37°C and then determining the remaining

infectious particles using plaque assay. Virus inactivation as determined by plaque assay readout demonstrated an even faster inactivation of influenza viruses by NCT compared to SARS-CoV-2. All tested virus strains were inactivated rapidly with a 2 $\log_{10}$ reduction of the H3N2 virus within 5 min (Fig. 3a) and a 6 $\log_{10}$ reduction of H1N1 and H1N1pdm viruses within 1 min by 1.0% NCT (Fig. 3b and 3c). In general, H1N1 and H1N1pdm viruses were more susceptible than the H3N2 virus. Addition of ammonium chloride (NH_4Cl) to NCT significantly enhanced its activity against influenza viruses (Fig. 3d). Ammonium chloride alone and the inactivation control with 0.1% NCT plus 0.1% ammonium chloride showed no antiviral effect at least up to 10 min incubation time.

Virucidal activity of NCT against RSV

Inactivation of RSV was assessed as described for SARS-CoV-2 and influenza A viruses. As with SARS-CoV-2 and influenza A virus, inactivation of RSV as determined by plaque assay readout demonstrated a significant reduction of PFU/ml by NCT compared to mock treated controls. The incubation of RSV with 1.0% NCT resulted in a rapid drop of infectious virus titre with 4 $\log_{10}$ decrease within 5 minutes (Fig. 4). Almost no detectable amount of infectious RSV was measurable after 15 minutes. In the presence of 0.1% NCT, RSV titres dropped in a time- and concentration-dependent manner reaching significant titre reduction after 15 minutes (Fig. 4).

Addition of 5% peptone to tests with 1% NCT and 0.5% peptone to 0.1% NCT did not enhance or decrease the virucidal activity but led to similar results as NCT without peptone (Suppl. Fig. 1). Addition of 5% peptone to the test with 0.1% NCT, however, led to inactivation of NCT, indicating a predominance of reduction of the active chlorine (Suppl. Fig. 1).

Structural changes of Coronavirus SARS-CoV-2 spike protein by NCT evaluated by mass spectrometry

Multiple sites of oxidative attack by NCT could be demonstrated by mass spectrometry. Chlorination of aromatic amino acids was found, in detail of 18 tyrosines, two phenylalanines, and one tryptophan. Two methionines were oxidized. The exact positions of the chlorinated and oxidized amino acids are illustrated in Fig. 5. No oxidation of cysteine could be detected.

Structural changes of Coronavirus 3C-like proteinase by NCT evaluated by mass spectrometry

As with spike protein, multiple sites of oxidative attack by NCT could be demonstrated. Chlorination of aromatic amino acids was found, in detail of 3 tyrosines, and two histidines. Seven methionines and four cysteines were oxidized. The exact positions of the chlorinated and oxidized amino acids are illustrated in Fig. 6.

Structural changes of hemagglutinin and neuraminidase of influenza and fusion glycoprotein of RSV by NCT evaluated by mass spectrometry

Also with these proteins of influenza and RSV, respectively, multiple chlorinations of tyrosines and oxidations of methionines and cysteines were detacted. Details are shown in Suppl. Fig. 2-4.

Discussion

Safe, well tolerated, affordable, and effective medications are urgently needed against COVID-19 and would be beneficial for treatment of viral bronchopneumonia caused by other viruses such as influenza and RSV. As an endogenous mild long-lived oxidant [17], inhaled NCT has been demonstrated to be well tolerated and safe in animals (pigs and mice) and in a clinical phase I study in humans [16,34-36]. As an active chlorine compound belonging to the class of chloramines, it has broad-spectrum activity against pathogens without occurrence of resistance because of the oxidizing mechanism of activity with thio- and amino-groups as the main targets [14,22,23,43,44].

Actually, in the present study NCT had clear virucidal activity against three enveloped RNA viruses highly relevant for infections of the bronchopulmonary system. Depending on the NCT-concentration and test conditions, a rapid reduction of the number of infectious virus particles by several powers of ten within 1 - 10 minutes is achieved. Influenza A viruses of pre-pandemic and pandemic H1N1 subtype (H1N1 and H1N1pdm) were the most sensitive ones with reduction to the detection limit by 1.0% NCT within 1 min, followed by RSV, influenza (H3N2), and SARS-CoV-2. These differences can be explained by individual dynamics of oxidation and chlorination of proteins of the viral surface, and of penetration of NCT and attack on the viral nucleocapsid proteins. All these target sites have been shown with the NCT analogue *N,N*-dichloro-2,2-dimethyltaurine in adenovirus type 5 [45]. Thereby, chlorination of the surface proteins is the first step [46], which can be assumed to impact their function and therefore the attachment of viruses to body cells. The multiple sites of chlorination of tyrosine, phenylalanine, and tryptophan and oxidation of methionine by NCT in the spike protein found in the present study clearly confirm this principle in SARS-CoV-2, too. Further targets are generally mainly thio groups and amino groups [22,43,44]. Actually, we found oxidation of cysteine and methionine in the 3C-like proteinase of the virus besides chlorination of tyrosine and histidine, which underlines the attack of NCT at multiple proteins. This is definitely confirmed by the multiple chlorinations and oxidations at similar

target amino acids of the tested proteins of influenza and RSV. Despite the occurrence of 40 cysteines in the spike protein (Fig. 5), no oxidation of them by NCT could be detected. A realistic explanation may be that they cannot be reached by NCT within the protein, which is underlined by their occurrence in part as disulfides (cystine).

Oxidation and chlorination of virulence factors of different pathogens by NCT and analogue chloramines with the consequence of their inactivation has been also shown for shigatoxin of *Escherichia coli [47]*, several toxins of *Staphylococcus aureus* [48], aspartyl proteinases of *Candida spp*. and gliotoxin of *Aspergillus fumigatus* [49,50]. This indicates that inactivation of key proteins of all kinds of pathogens is a central principle of the antimicrobial action of NCT and may underline such a function in innate immunity besides its anti-inflammatory one [15,20,23].

Accordingly, the activity of NCT against the SARS-CoV-2 variants of concern was almost identical to that against the wild type. This expected result means that mutations in the protein sequence have no influence on the susceptibility of the virus to NCT. Similarly, multiresistance of bacteria and fungi against antibiotics and antifungals does not play a role for their susceptibility to NCT [51,52]. As a further consequence, NCT has not only virucidal activity against enveloped viruses (herpes virus type 1 and 2 [26,27], human immunodeficiency virus 1 [28], and the viruses of the present study), but also non-enveloped ones. From the latter, a panel of adenoviruses has been tested mainly due to their importance in epidemic keratoconjunctivitis [25,27,30]. Similar to other active halogen compounds and other antiseptics such as tensidic compounds [53], adenoviruses are slightly less sensitive to NCT than the enveloped viruses [27]. Nevertheless, efficacy of NCT *in vivo* against adenoviruses in epidemic keratoconjunctivitis has been proven in the New Zealand White rabbit ocular model and in a phase II study in humans [30,31]. Application of NCT had a curative effect in a patient suffering from therapy-refractory herpes zoster infection in the upper thoracic area [29].

It must be taken into account that organic substances are omnipresent *in vivo* (in all human body fluids and tissues), and therefore we performed a part of the inactivation assays in the presence of organic matter as well. The results of Fig. 2a clearly show an enhancement of the virucidal activity of NCT in the presence of 5.0% peptone, which in the first view appears surprising since active chlorine compounds underlie a decrease of their oxidation capacity by chlorine-reducing substances of such organic load [23,54,55]. With NCT as a low-reactive chloramine compound, however, transchlorination as one of the reaction mechanisms becomes important [14,23]. Thereby, amongst others, monochloramine (NH_2Cl) is formed in equilibrium from NCT and ammonium chloride [14,17].

$$Cl\text{-}HN\text{-}CH_2\text{-}CH_2\text{-}SO_3^- + NH_4Cl \leftrightarrow H_2N\text{-}CH_2\text{-}CH_2\text{-}SO_3^- + NH_2Cl + H^+ + Cl^-$$

NCT + ammonium chloride ↔ taurine + monochloramine

Monochloramine is more lipophilic than NCT and penetrates microorganisms more easily, which leads to enhanced inactivation by the reaction just mentioned [17,56]. The stronger activity of NCT in the presence of fluids containing proteinaceous material is a general principle observed in different compositions, such as artificial sputum medium, different body fluids, peptone, and plasma for bacteria and fungi (for review see [14,24,57]). In the present study, it has been confirmed for viruses for the first time, too. The discrepancy between the incubation time of 15 min (Fig. 2a) and of 10 min or less (Fig. 2b-e) needed for a significant viral reduction in buffer solution in different tests may be explained by the presence of 1.0% FCS in the tests depicted in Fig. 2c-e and organic matter in the presence of Vero cells in Fig. 2b. In agreement with these results, enhancement of the bactericidal and fungicidal activity of NCT in the presence of different lung epithelial cells was observed recently [33].

Tests with RSV, where the final concentration of organic matter was 50% DMEM and 0.5% FCS, disclosed rapid killing by NCT, too. Addition of peptone to this solution did not

further increase the activity, but disclosed that a high protein load of 5% inactivates a relatively low concentration of 0.1% NCT. This is explained by reduction of the oxidation capacity by the proportion of reducing molecules in peptone, which outweighs the transchlorination effects when NCT is too low concentrated [47,57]. As a practical consequence, a sufficient concentration of NCT, usually 1%, should be used for clinical application (e.g. [14,16,24]).

Enhancement of antimicrobial and antiviral activity by organic material is of practical relevance for topical treatment of infections with NCT, for instance bronchopulmonary ones. The concentration of active chlorine after the end of an inhalation of 1.0% NCT decreases to traces within 1 min and vanishes completely after further 10 min [16]. Inhalation for 10 min is feasible and well tolerated, and within this time an impact on SARS-CoV-2 and on other viruses can be expected *in vivo*, too, but remains to be evaluated in respective clinical studies.

Also of practical relevance is the fact that NCT has broad-spectrum activity against viruses, including important representatives relevant for bronchopulmonary infections (SARS-CoV-2, influenza viruses, RSV). Of note, even different variants of the viruses with concerning phenotypes such as increased spread or virulence are similarly susceptible due to the unspecific, oxidizing and chlorinating mechanism of action of NCT. Topical treatment of all these virus infections by inhaled NCT without the necessity of a diagnosis of the specific virus at hand is conceivable and should urgently be investigated in clinical studies. Notably, the activity of NCT against bacteria and fungi, including multi-resistant ones, may prevent super- and secondary infections, which are a considerable problem in COVID-19 patients as well [9-11]. In addition, the anti-inflammatory activity of NCT might have the potential to influence the aggressive inflammatory response by downregulating the “cytokine storm” and prevent airway damage in severe ill patients with SARS-CoV-2 infection. Further advantages of NCT would be high safety and high tolerability by human tissue [14], absence of systemic absorption, of systemic adverse effects [16], of systemic interaction with other medications,

and of resistance development because of the oxidizing and chlorinating mechanism of action [14,23].

Conclusions

NCT demonstrated rapid activity against SARS-CoV-2, influenza A viruses, and RSV at a therapeutic concentration of 1.0% that can be safely inhaled. The molecular mechanism of action consists of oxidative attack at multiple sites of essential viral proteins, which excludes development of resistance and maintains virucidal activity against virus variants. The activity is enhanced by an organic environment, which is omnipresent in human body fluids and tissues *in vivo*. Clinical efficacy of NCT in viral bronchopulmonary infections should be investigated in respective clinical studies.

Acknowledgments

We are grateful to Andrea Windisch for excellent technical assistance in the production of NCT and to Thomas Grunwald and Leila Issmail, Fraunhofer Institute for Cell Therapy and Immunology, Leipzig, Germany, for provision of and technical support with the RSV. We thank Brian Monk (Otago University, Dunedin, New Zealand) and Ian Monk (Doherty Institute, Melbourne, Australia) for establishing the connection with 360biolabs, Melbourne, Australia.

Declaration of interest statement

M. Nagl is co-inventor of a patent on the application of NCT for inhalation (EP 2265267 B1). All other authors declare no conflict of interest.

Funding

This study was supported by the German Federal Ministry of Education and Research (BMBF) grants “NUM Organo-Strat” and “BUA Coronavirus Exploration project”.

Author Contributions

A.R., A.V., M.S., T.W., A.L., J.F. and H.S. performed the assays against SARS-CoV-2, M.S., T.W., J.S. and M.N. the assays against influenza viruses, B.M. and Z.B. the assays against RSV. P.T. and M.N. planned the investigations with the spike protein. L.K. and B.S. planned and performed the mass spectrometry. M.L., M.N., C.S., D.v.L., and P.T. planned the work, made the concept and guided the work. M.N. and M.L. wrote the manuscript under contribution of all other authors. All authors edited and approved the manuscript.

References

1. Dhama K, Khan S, Tiwari R, et al. Coronavirus Disease 2019-COVID-19. Clinical microbiology reviews. 2020 Sep 16;33(4).
2. Malik YS, Kumar N, Sircar S, et al. Coronavirus Disease Pandemic (COVID-19): Challenges and a Global Perspective. Pathogens (Basel, Switzerland). 2020 Jun 28;9(7).
3. Fierabracci A, Arena A, Rossi P. COVID-19: A Review on Diagnosis, Treatment, and Prophylaxis. International journal of molecular sciences. 2020 Jul 21;21(14).
4. World Health Organization. Influenza (Seasonal) [website]. World Health Organization; 2018 [updated 2018/11/06]. Available from: https://www.who.int/news-room/fact-sheets/detail/influenza-(seasonal)
5. Smith DJ, Lapedes AS, de Jong JC, et al. Mapping the antigenic and genetic evolution of influenza virus. Science. 2004 Jul 16;305(5682):371-6.
6. Mitchell JP, Berlinski A, Canisius S, et al. Urgent Appeal from International Society for Aerosols in Medicine (ISAM) During COVID-19: Clinical Decision Makers and Governmental Agencies Should Consider the Inhaled Route of Administration: A Statement from the ISAM Regulatory and Standardization Issues Networking Group. J Aerosol Med Pulm Drug Deliv. 2020 Aug;33(4):235-238.
7. Arentz M, Yim E, Klaff L, et al. Characteristics and Outcomes of 21 Critically Ill Patients With COVID-19 in Washington State. Jama. 2020 Mar 19.

8. Zhou F, Yu T, Du R, et al. Clinical course and risk factors for mortality of adult inpatients with COVID-19 in Wuhan, China: a retrospective cohort study. Lancet. 2020 Mar 11.
9. Arastehfar A, Carvalho A, van de Veerdonk FL, et al. COVID-19 Associated Pulmonary Aspergillosis (CAPA)-From Immunology to Treatment. Journal of fungi (Basel, Switzerland). 2020 Jun 24;6(2).
10. Koehler P, Cornely OA, Böttiger BW, et al. COVID-19 associated pulmonary aspergillosis. Mycoses. 2020 Jun;63(6):528-534.
11. Zhu X, Ge Y, Wu T, et al. Co-infection with respiratory pathogens among COVID-2019 cases. Virus Res. 2020 Aug;285:198005.
12. Aufklärung Bfg. Test auf eine Infektion mit dem Coronavirus SARS-CoV-2 2020 [cited 2020 06/11/2020]. Available from: https://www.infektionsschutz.de/coronavirus/basisinformationen/test-auf-sars-cov-2.html#c13339
13. Ye Q, Wang B, Mao J. Cytokine Storm in COVID-19 and Treatment. The Journal of infection. 2020 Apr 10.
14. Gottardi W, Nagl M. N-chlorotaurine, a natural antiseptic with outstanding tolerability. J Antimicrob Chemother. 2010 2010;65(3):399-409.
15. Marcinkiewicz J, Kontny E. Taurine and inflammatory diseases. Amino Acids. 2014 2014;46(1):7-20.
16. Arnitz R, Stein M, Bauer P, et al. Tolerability of inhaled N-chlorotaurine in humans – a double-blind randomized phase I clinical study. Ther Adv Resp Dis. 2018;12:1-14.
17. Grisham MB, Jefferson MM, Melton DF, et al. Chlorination of endogenous amines by isolated neutrophils. J Biol Chem. 1984 1984;259(16):10404-10413.
18. Weiss SJ, Klein R, Slivka A, et al. Chlorination of taurine by human neutrophils. J Clin Investig. 1982 1982;70(3):598-607.
19. Zgliczynski JM, Stelmaszynska T, Domanski J, et al. Chloramines as intermediates of oxidation reaction of amino acids by myeloperoxidase. Biochim Biophys Acta. 1971 6/16/1971;235(3):419-424.
20. Kim C, Cha YN. Taurine chloramine produced from taurine under inflammation provides anti-inflammatory and cytoprotective effects. Amino Acids. 2014 1/2014;46(1):89-100.
21. Park E, Alberti J, Quinn MR, et al. Taurine chloramine inhibits the production of superoxide anion, IL-6 and IL-8 in activated human polymorphonuclear leukocytes. Adv Exp Med Biol. 1998 1998;442:177-182.
22. Gottardi W, Nagl M. Chemical properties of N-chlorotaurine sodium, a key compound in the human defence system. Arch Pharm Pharm Med Chem. 2002 9/2002;335(9):411-421.
23. Gottardi W, Debabov D, Nagl M. N-chloramines: a promising class of well-tolerated topical antiinfectives. Antimicrob Agents Chemother. 2013 2013;57(3):1107-1114.
24. Nagl M, Arnitz R, Lackner M. *N*-chlorotaurine, a promising future candidate for topical therapy of fungal infections. Mycopathologia. 2018 2018;183(1):161-170.
25. Garcia LAT, Boff L, Barardi CRM, et al. Inactivation of adenovirus in water by natural and synthetic compounds Food and Environmental Virology. 2019;11(2):157-166.
26. Huemer HP, Nagl M, Irschick EU. In vitro prevention of vaccinia and herpes virus infection spread in explanted human corneas by N-chlorotaurine. Ophthalmic Res. 2010 2010;43(3):145-152.
27. Nagl M, Larcher C, Gottardi W. Activity of N-chlorotaurine against herpes simplex- and adenoviruses. Antiviral Res. 1998 1998;38(1):25-30.

28. Dudani AK, Martyres A, Fliss H. Short communication: rapid preparation of preventive and therapeutic whole-killed retroviral vaccines using the microbicide taurine chloramine. AIDS Res Hum Retroviruses. 2008 4/2008;24(4):635-642.
29. Kyriakopoulos AM, Logotheti S, Marcinkiewicz J, et al. N-chlorotaurine and N-bromotaurine combination regimen for the cure of valacyclovir-unresponsive herpes zoster comorbidity in a multiple sclerosis patient. International Journal of Medical and Pharmaceutical Case Reports. 2016 2016;7(2):1-6.
30. Romanowski EG, Yates KA, Teuchner B, et al. N-chlorotaurine is an effective antiviral agent against adenovirus in vitro and in the Ad5/NZW rabbit ocular model. Invest Ophthalmol Vis Sci. 2006 2006;47(5):2021-2026.
31. Teuchner B, Nagl M, Schidlbauer A, et al. Tolerability and efficacy of N-chlorotaurine in epidemic keratoconjunctivitis – a double-blind randomized phase 2 clinical trial. J Ocul Pharmacol Ther. 2005 2005;21(2):157-165.
32. Jekle A, Abdul RS, Celeri C, et al. Broad-spectrum virucidal activity of (NVC-422) N,N-dichloro-2,2-dimethyltaurine against viral ocular pathogens in vitro. Invest Ophthalmol Vis Sci. 2013 2/2013;54(2):1244-1251.
33. Leiter H, Toepfer S, Messner P, et al. Microbicidal activity of N-chlorotaurine can be enhanced in the presence of lung epithelial cells Journal of Cystic Fibrosis. 2020.
34. Geiger R, Treml B, Pinna A, et al. Tolerability of inhaled N-chlorotaurine in the pig model. BMC Pulmon Med. 2009 2009;9(1):33.
35. Nagl M, Eitzinger C, Dietrich H, et al. Tolerability of inhaled N-chlorotaurine versus sodium chloride in the mouse. J Med Res Pract. 2013 2013;2(6):163-170.
36. Schwienbacher M, Treml B, Pinna A, et al. Tolerability of inhaled N-chlorotaurine in an acute pig streptococcal lower airway inflammation model. BMC Infect Dis. 2011 2011;11:231.
37. Böttcher B, Sarg B, Lindner HH, et al. Inactivation of microbicidal active halogen compounds by sodium thiosulphate and histidine/methionine for time-kill assays. J Microbiol Methods. 2017;141:42-47.
38. Hoffmann M, Kleine-Weber H, Schroeder S, et al. SARS-CoV-2 Cell Entry Depends on ACE2 and TMPRSS2 and Is Blocked by a Clinically Proven Protease Inhibitor. Cell. 2020 Apr 16;181(2):271-280.e8.
39. Ternette N, Tippler B, Uberla K, et al. Immunogenicity and efficacy of codon optimized DNA vaccines encoding the F-protein of respiratory syncytial virus. Vaccine. 2007 Oct 10;25(41):7271-9.
40. Reed LJ, Muench H. A simple method of estimating fifty percent endpoints. American Journal of Epidemiology. 1938;27(3):493-497.
41. Shatzkes K, Teferedegne B, Murata H. A simple, inexpensive method for preparing cell lysates suitable for downstream reverse transcription quantitative PCR. Scientific reports. 2014 Apr 11;4:4659.
42. Corman VM, Landt O, Kaiser M, et al. Detection of 2019 novel coronavirus (2019-nCoV) by real-time RT-PCR. Euro surveillance : bulletin Europeen sur les maladies transmissibles = European communicable disease bulletin. 2020 Jan;25(3).
43. Fernandez MI, Garcia MV, Armesto XL, et al. Unravelling the mechanism of intracellular oxidation of thiols by (N-Cl)-Taurine. Journal of Physical Organic Chemistry. 2013 2013;26(12):1098-1104.
44. Peskin AV, Winterbourn CC. Taurine chloramine is more selective than hypochlorous acid at targeting critical cysteines and inactivating creatine kinase and glyceraldehyde-3-phosphate dehydrogenase. Free Radic Biol Med. 2006 1/1/2006;40(1):45-53.
45. Yoon J, Jekle A, Najafi R, et al. Virucidal mechanism of action of NVC-422, a novel antimicrobial drug for the treatment of adenoviral conjunctivitis. Antiviral Res. 2011 10/15/2011;92(3):470-478.

46. Gottardi W, Nagl M. Chlorine covers on living bacteria: the initial step in antimicrobial action of active chlorine compounds. J Antimicrob Chemother. 2005 2005;55(4):475-482.
47. Eitzinger C, Ehrlenbach S, Lindner H, et al. N-chlorotaurine, a long-lived oxidant produced by human leukocytes, inactivates Shiga toxin of enterohemorrhagic *Escherichia coli*. PloS One. 2012 2012;7(11):e47105.
48. Jekle A, Yoon J, Zuck M, et al. NVC-422 inactivates *Staphylococcus aureus* toxins. Antimicrob Agents Chemother. 2013 2013;57(2):924-929.
49. Nagl M, Gruber A, Fuchs A, et al. Impact of N-chlorotaurine on viability and production of secreted aspartyl proteinases of *Candida* spp. Antimicrob Agents Chemother. 2002 2002;46(6):1996-1999.
50. Reeves EP, Nagl M, O'Keeffe J, et al. Effect of N-chlorotaurine on *Aspergillus*, with particular reference to destruction of secreted gliotoxin. J Med Microbiol. 2006 7/2006;55(Pt 7):913-918.
51. Anich C, Orth-Höller D, Lackner M, et al. Microbicidal activity of N-chlorotaurine against multiresistant nosocomial bacteria. J Appl Microbiol. 2021:DOI: 10.1111/jam.15052.
52. Lackner M, Binder U, Reindl M, et al. N-chlorotaurine exhibits fungicidal activity against therapy-refractory *Scedosporium species* and *Lomentospora prolificans*. Antimicrob Agents Chemother. 2015 2015;59(10):6454-6462.
53. Sauerbrei A, Sehr K, Brandstadt A, et al. Sensitivity of human adenoviruses to different groups of chemical biocides. J Hosp Infect. 2004 5/2004;57(1):59-66.
54. Kramer A, Dissemond J, Kim S, et al. Consensus on Wound Antisepsis: Update 2018. Skin pharmacology and physiology. 2018;31(1):28-58.
55. McDonnell G, Russell AD. Antiseptics and disinfectants: activity, action, and resistance. Clin Microbiol Rev. 1999 1/1999;12(1):147-179.
56. Gottardi W, Arnitz R, Nagl M. N-chlorotaurine and ammonium chloride: an antiseptic preparation with strong bactericidal activity. Int J Pharm. 2007 2007;335(1-2):32-40.
57. Gruber M, Moser I, Nagl M, et al. Bactericidal and fungicidal activity of N-chlorotaurine is enhanced in cystic fibrosis sputum medium. Antimicrob Agents Chemother. 2017 2017;61(5):1-10.

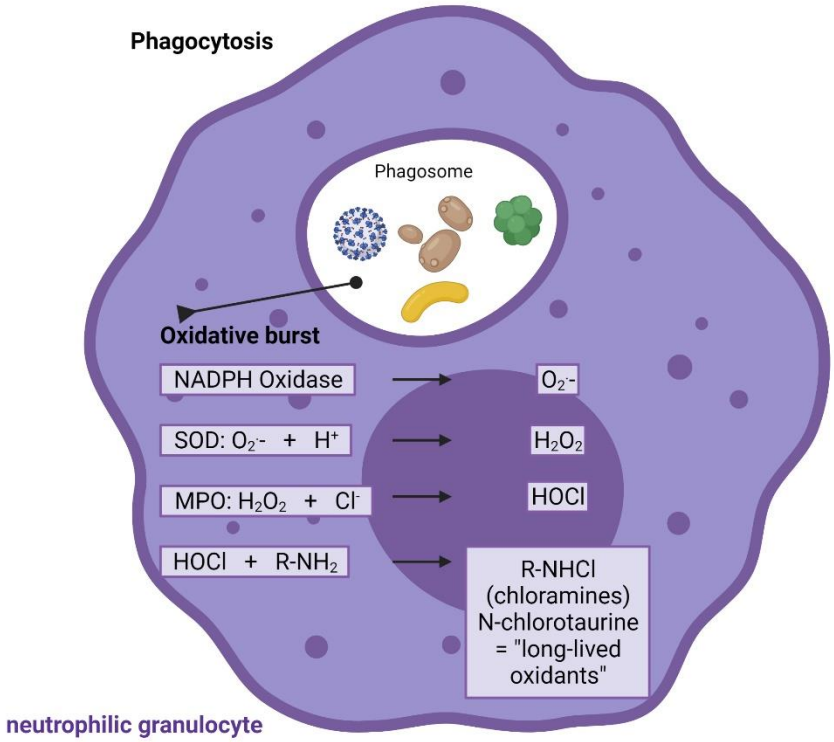

Fig. 1: Endogenous origin of NCT. NCT is formed in activated human granulocytes and monocytes via an enzymatic cascade, the oxidative burst. Subsequent to superoxide ($O_2^{\cdot-}$) and hydrogen peroxide (H_2O_2), the highly reactive hypochlorite (HOCl) is created by myeloperoxidase (MPO), which among others reacts with amino compounds to form less reactive chloramines, also named long-lived oxidants. NCT is the main representative of these chloramines. SOD superoxide dismutase. Fig. 1 was made in ©BioRender - biorender.com

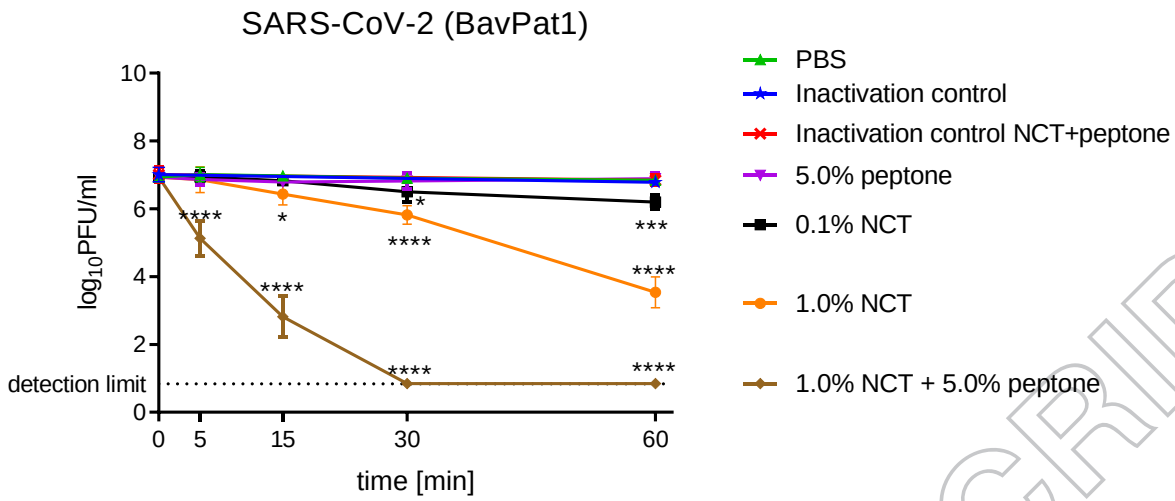

Fig. 2: Inactivation of SARS-CoV-2 by NCT. a, Virus suspension (SARS-CoV-2 BavPat1) was incubated with 1.0% (55 mM) NCT, 0,1% (5.5 mM) NCT, 1.0% NCT with 5.0% peptone or PBS or 5.0% peptone for 5 min, 15 min, 30 min, or 60 min at 37°C, after which samples were diluted 1:1 in met/his solution for inactivation of NCT. Remaining infectious virus particles were determined using plaque titration. To control for inactivation of NCT by met/his, virus was added after dilution of 1.0% NCT with or without peptone in met/his. Mean values ± SD of three to eight independent experiments in duplicates. The dotted line indicates the detection limit (0.84 $\log_{10}$). Data were statistically analysed using a two-way ANOVA including a Dunnett's multiple comparison test to PBS controls. * $p < 0.05$, ** $p < 0.01$, *** $p < 0.001$, **** $p < 0.0001$. Of note, the inactivation of the virus by NCT was markedly enhanced in the presence of peptone.

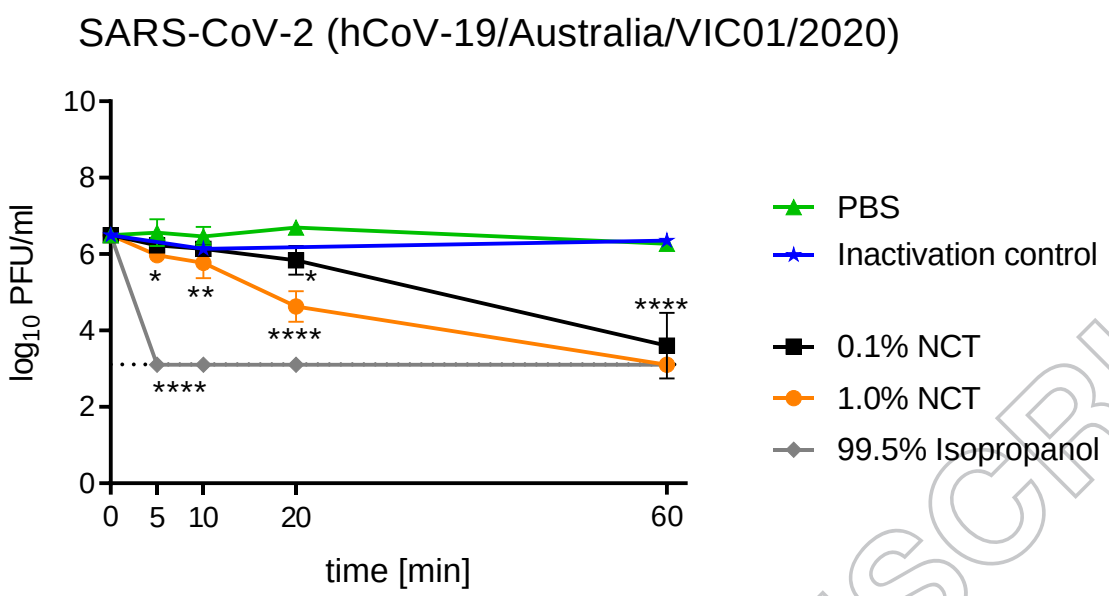

Fig. 2: Inactivation of SARS-CoV-2 by NCT. b, Virus suspension (SARS-CoV-2 h CoV-19/Australia/VIC01/2020) was incubated with NCT or PBS or isopropanol (positive control) for 5 min, 10 min, 20 min, and 60 min at 37°C and then diluted 1:1 in met/his for inactivation of NCT, followed by plaque titration. Mean values ± SD of three independent experiments. Detection limit 3.11 $\log_{10}$ (dotted line).

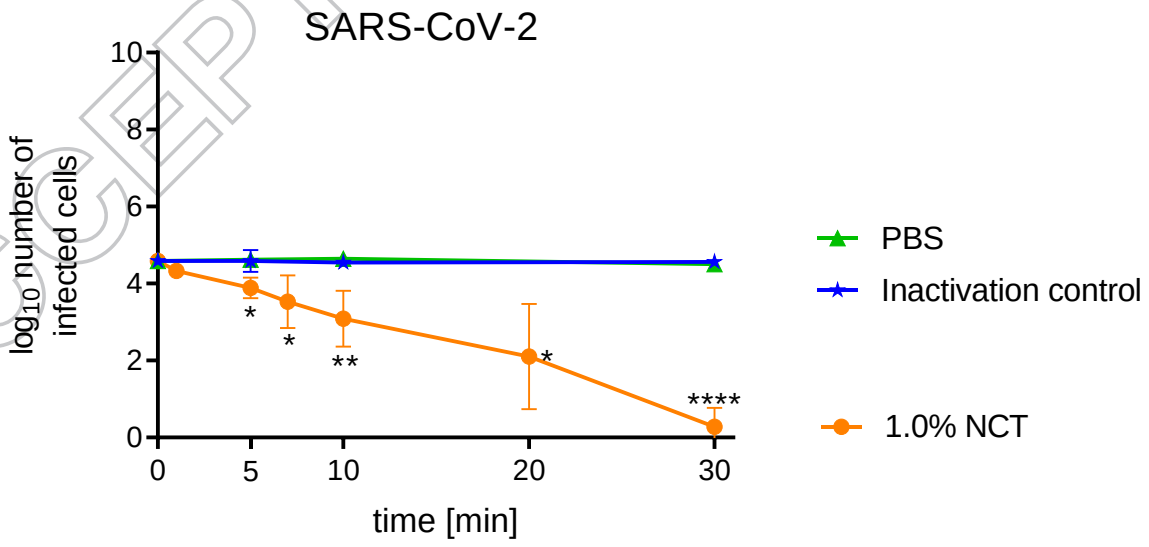

Fig. 2: Inactivation of SARS-CoV-2 by NCT. **c**, Virus suspension (SARS-CoV-2, clinical isolate) was incubated with 1% NCT or PBS for 1 min, 5 min, 7 min, 10 min, 20 min, and 30 min at 37°C. After inactivation of NCT and serial dilution, aliquots were added to Vero/TMPRSS2/ACE2 cells for 1 h in 96-well plates. Cells were washed, incubated for further 9 h, and fixed for Immunostaining (**c**) or RT-qPCR (**d**). In immunostaining, infected cells were visible as red spots and counted using an ImmunoSpot S6 Ultra-V reader and CTL analyser *BioSpot*® 5.0 software. Mean values ± SD of three independent experiments.

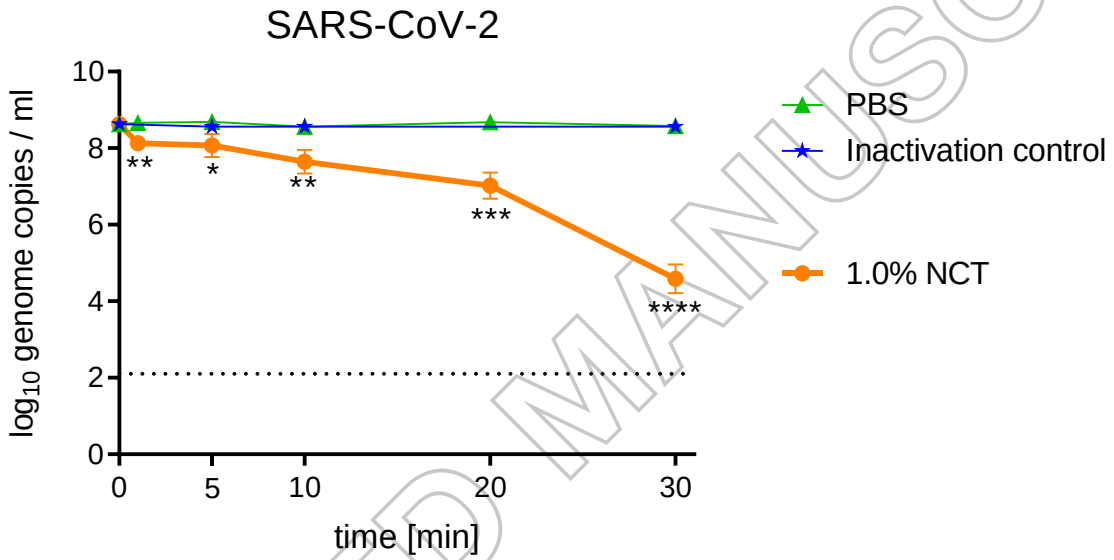

Fig. 2: Inactivation of SARS-CoV-2 by NCT. d, After cell lysis and RNA extraction, one-step RT-qPCR assay was performed using the iTaq™ RT-PCR (BIO-RAD) kit and previously published primers and probes specific for detection of the SARS-CoV-2 E Gene on a CFX96™ real-time system (BIO-RAD). Mean values ± SD of genome copies of three independent experiments. Detection limit 2.10 $\log_{10}$ RNA copies/ml (dotted line).

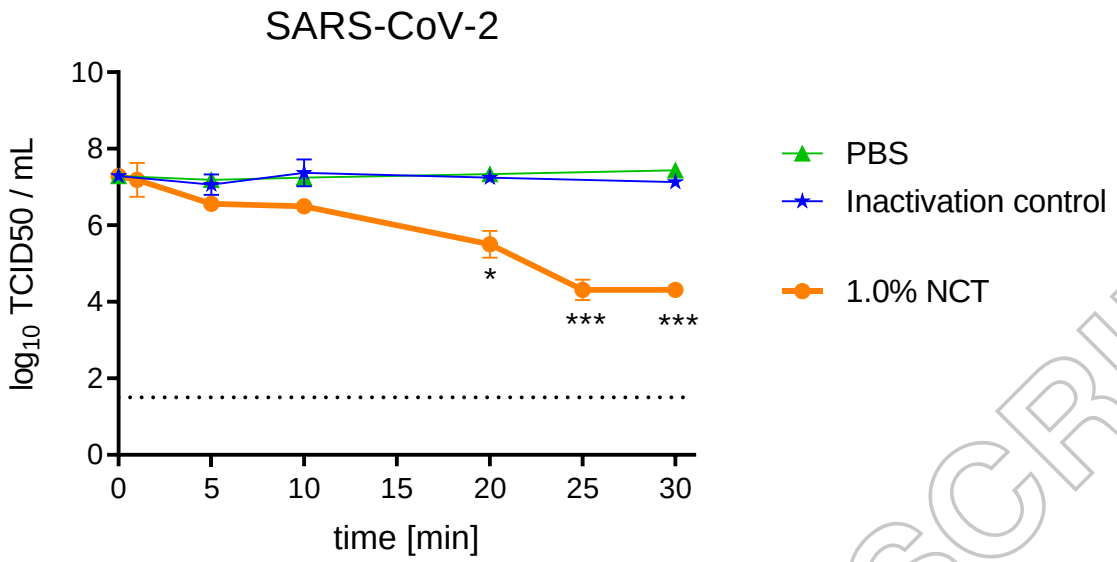

Fig. 2: Inactivation of SARS-CoV-2 by NCT. e, Virus titration by $TCID_{50}$. Mean values ± SD of two independent experiments. Detection limit 1.50 log_{10} (dotted line).

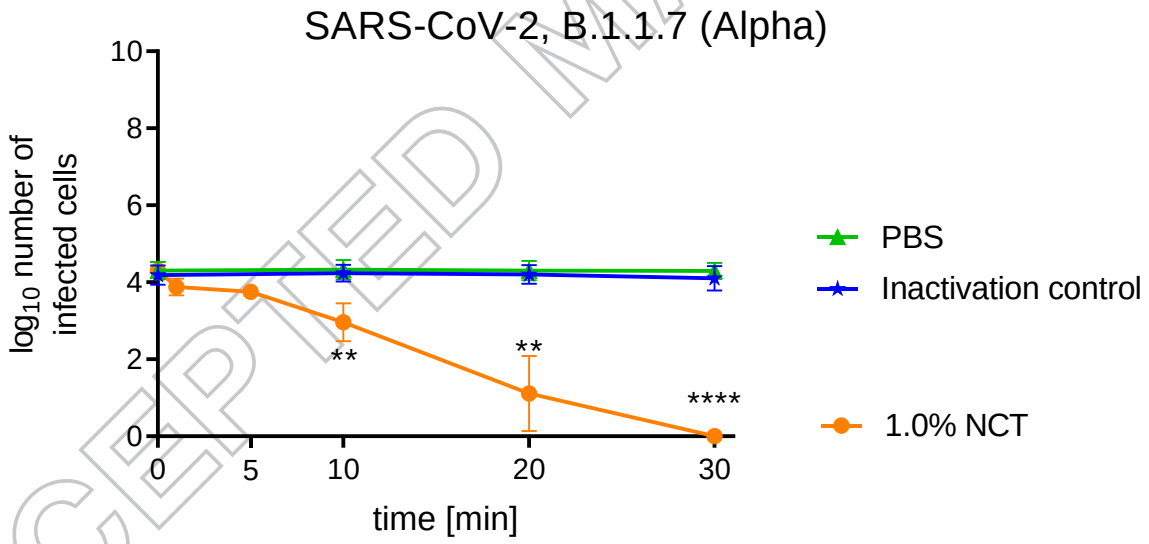

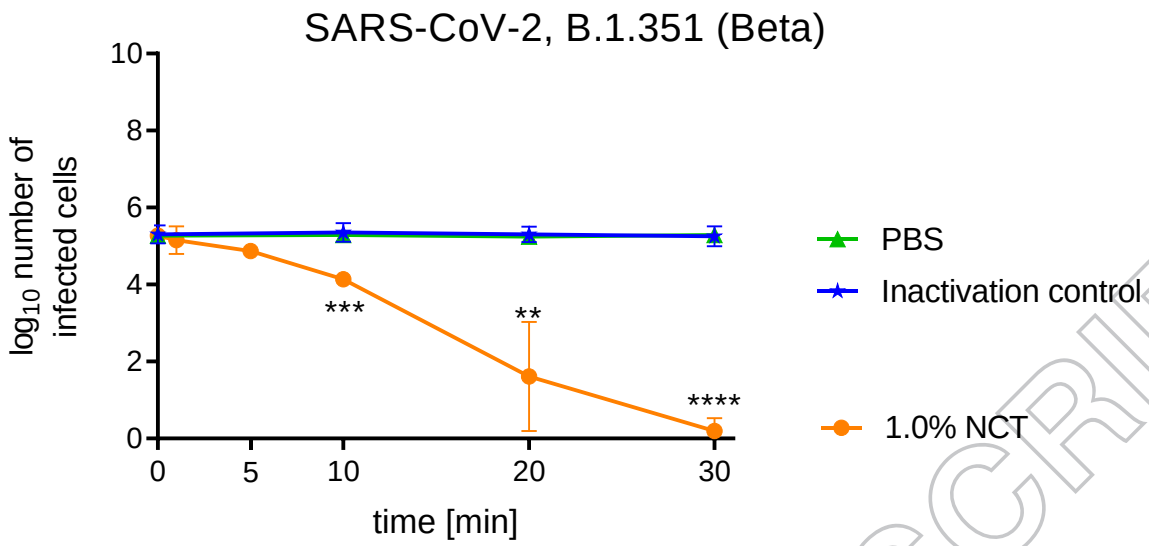

Fig. 2: Inactivation of SARS-CoV-2 by NCT. f,g, Virus suspension (SARS-CoV-2 variants, i.e. B.1.1.7 (Alpha) (**f**), B.1.351 (Beta) (**g**)) was incubated with 1% NCT or PBS for 1 min, 5 min, 10 min, 20 min, and 30 min at 37°C. After inactivation of NCT and serial dilution, aliquots were added to Vero/TMPRSS2/ACE2 cells for 1 h in 96-well plates. Cells were washed, incubated for further 9 h, and fixed for Immunostaining. Infected cells were visible as red spots and counted using an ImmunoSpot S6 Ultra-V reader and CTL analyser *BioSpot*® 5.0 software. Mean values ± SD of three independent experiments.

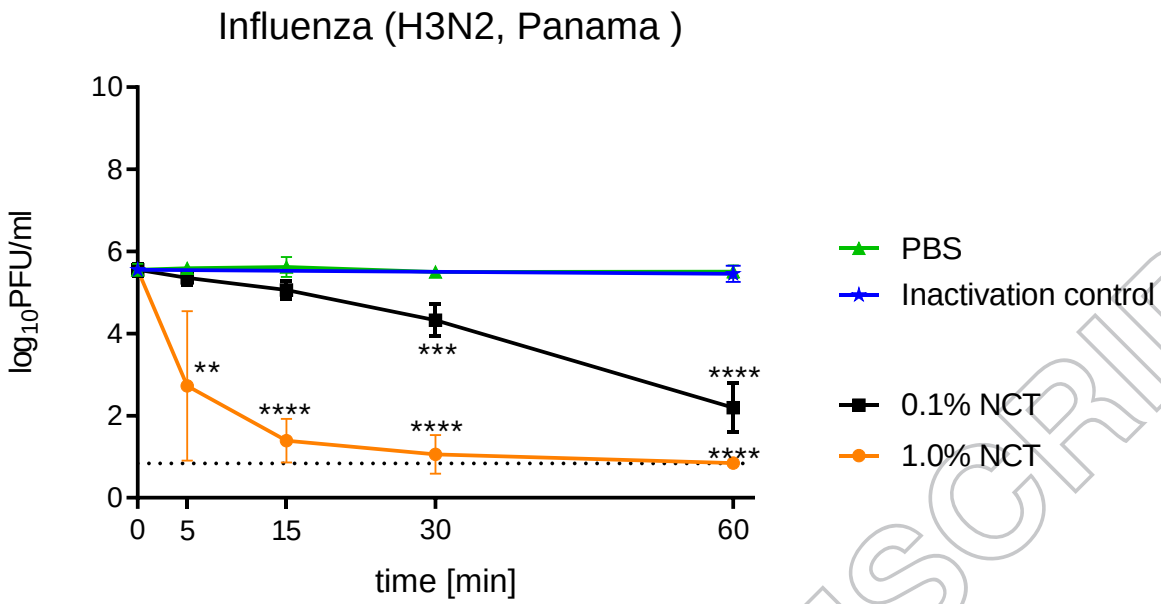

Fig. 3: Inactivation of influenza viruses by NCT. a, Inactivation of Influenza A/Panama/2007/1999 (H3N2) by 1.0% (55 mM) and 0.1% (5.5 mM) NCT. Virus suspension was incubated with NCT or PBS for 5 min, 15 min, 30 min, or 60 min at 37°C, after which samples were diluted 1:1 in met/his solution for inactivation of NCT. Remaining infectious virus particles were determined using plaque titration. To control for inactivation of NCT by met/his, virus was added after dilution of 1.0% NCT in met/his in the inactivation control. Mean values ± SD of five independent experiments. * $p < 0.05$, ** $p < 0.01$, *** $p < 0.001$, **** $p < 0.0001$ versus PBS control. Detection limit 0.84 $\log_{10}$ (dotted line).

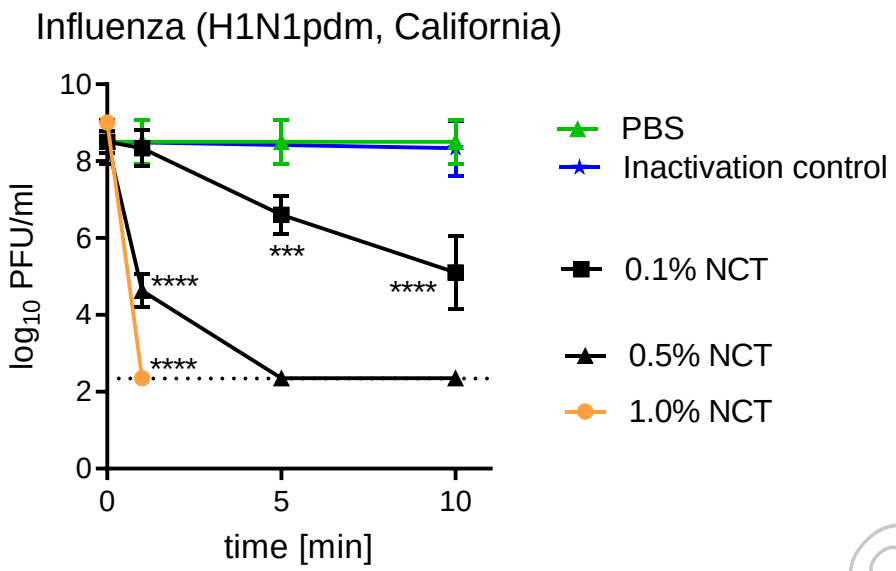

Fig. 3: Inactivation of influenza viruses by NCT. b, Inactivation of Influenza A/California/ Swine Origin Virus/2009 (H1N1pdm) by 0.1%, 0.5% and 1.0% NCT.

Virus suspension was incubated with NCT in RPMI or plain RPMI for 1 min, 5 min, and 10 min at 22°C, after which samples were diluted 1:1 in met/his solution for inactivation of NCT. Remaining infectious virus particles were determined using plaque titration. Mean values ± SD of four independent experiments. Detection limit 2.35 $\log_{10}$ (dotted line).

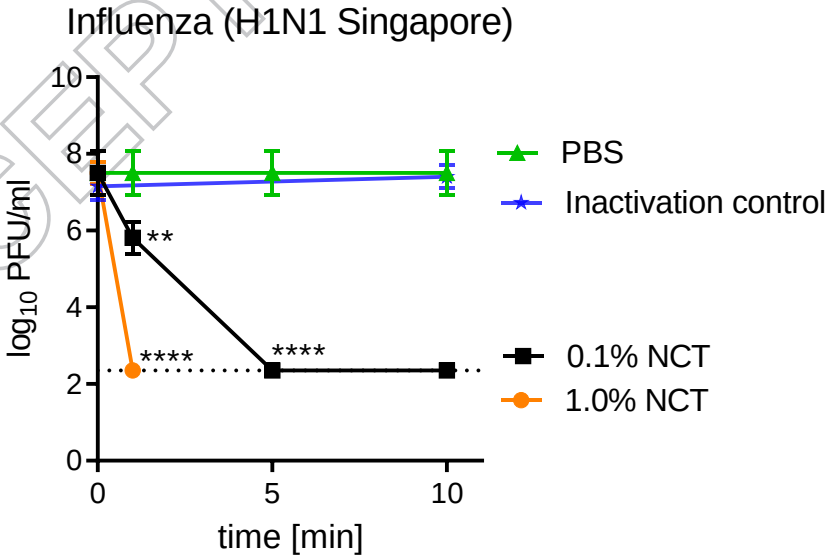

Fig. 3: Inactivation of influenza viruses by NCT. c, Inactivation of Influenza A/Singapore/Hongkong/2339/2000 (H1N1) by 0.1% and 1.0% NCT and (**d**) by 0.1% NCT and 0.1% (5.5 mM) NCT plus 0.1% (18.7 mM) ammonium chloride compared. Test procedure and number of independent experiments as in Fig. 3b.

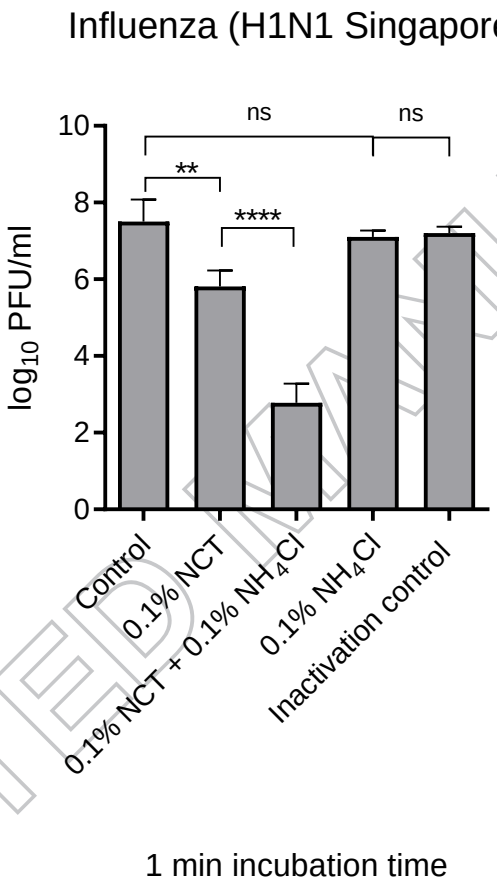

Fig. 3: Inactivation of influenza viruses by NCT. c, Inactivation of Influenza A/Singapore/Hongkong/2339/2000 (H1N1) by 0.1% and 1.0% NCT and (**d**) by 0.1% NCT and 0.1% (5.5 mM) NCT plus 0.1% (18.7 mM) ammonium chloride compared. Test procedure and number of independent experiments as in Fig. 3b. Inactivation control in (**d**) consisting of 0.1% NCT plus 0.1% NH_4Cl plus inactivator.

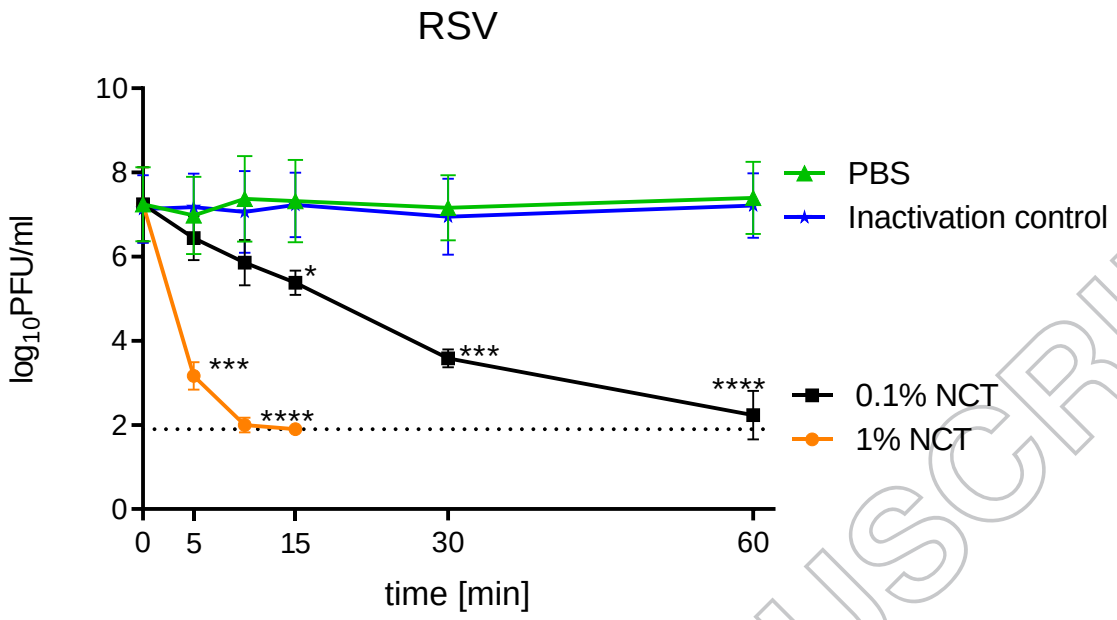

Fig. 4: Inactivation of respiratory syncytial virus by NCT. Virus suspension was incubated with 1.0% or 0.1% NCT or PBS for 5 min, 10 min, 15 min, 30 min, or 60 min at 37°C, after which samples were diluted 1:1 in met/his solution for inactivation of NCT. Remaining infectious virus particles were determined using plaque titration. Mean values ± SD of three independent experiments. Detection limit 1.90 $\log_{10}$ (dotted line).

UniProtKB – P0DTC2 (SPIKE_SARS2)

```
MFVFLVLLPL VSSQCVNLTT RTQLPPAYTN SFTRGVYYPD KVFRSSVLHS 50
TQDLFLPFFS NVTWFHAIHV SGTNGTKRFD NPVLPFNDGV YFASTEKSNI 100
IRGWIFGTTL DSKTQSLLIV NNATNVVIKV CEFQFCNDPF LGVYYHKNNK 150
SWMESEFRVY SSANNCTFEY VSQPFLMDLE GKQGNFKNLR EFVFKNIDGY 200
FKIYSKHTPI NLVRDLPQGF SALEPLVDLP IGINITRFQT LLALHRSYLT 250
PGDSSSGWTA GAAAYYVGYL QPRTFLLKYN ENGTITDAVD CALDPLSETK 300
CTLKSFTVEK GIYQTSNFRV QPTESIVRFP NITNLCPFGE VFNATRFASV 350
YAWNRKRISN CVADYSVLYN SASFSTFKCY GVSPTKLNDL CFTNVYADSF 400
VIRGDEVRQI APGQTGKIAD YNYKLPDDFT GCVIAWNSNN LDSKVGGNYN 450
YLYRLFRKSN LKPFERDIST EIYQAGSTPC NGVEGFNCYF PLQSYGFQPT 500
NGVGYQPYRV VVLSFELLHA PATVCGPKKS TNLVKNKCVN FNFNGLTGTG 550
VLTESNKKFL PFQQFGRDIA DTTDAVRDPQ TLEILDITPC SFGGVSVITP 600
GTNTSNQVAV LYQDVNCTEV PVAIHADQLT PTWRVYSTGS NVFQTRAGCL 650
```

IGAEHVNNSY ECDIPIGAGI CASYQTQTNS PRRARSVASQ SIIAYTMSLG 700
AENSVAYSNN SIAIPTNFTI SVTTEILPVS MTKTSVDCTM YICGDSTECS 750
NLLLQYGSFC TQLNRALTGI AVEQDKNTQE VFAQVKQIYK TPPIKDFGGF 800
NFSQILPDPS KPSKRSFIED LLFNKVTLAD AGFIKQYGDC LGDIAARDLI 850
CAQKFNGLTV LPPLLTDEMI AQYTSALLAG TITSGWTFGA GAALQIPFAM 900
QMAYRFNGIG VTQNVLYENQ KLIANQFNSA IGKIQDSLSS TASALGKLQD 950
VVNQNAQALN TLVKQLSSNF GAISSVLNDI LSRLDKVEAE VQIDRLITGR 1000
LQSLQTYVTQ QLIRAAEIRA SANLAATKMS ECVLGQSKRV DFCGKGYHLM 1050
SFPQSAPHGV VFLHVTYVPA QEKNFTTAPA ICHDGKAHFP REGVFVSNGT 1100
HWFVTQRNFY EPQIITTDNT FVSGNCDVVI GIVNNTVYDP LQPELDSFKE 1150
ELDKYFKNHT SPDVDLGDIS GINASVVNIQ KEIDRLNEVA KNLNESLIDL 1200
QELGKYEQYI KWPWYIWLGF IAGLIAIVMV TIMLCCMTSC CSCLKGCCSC 1250
GSCCKFDEDD SEPVLKGVKL HYT

Identified Peptide	**Position in Protein**	**Chlorination / Oxidation Site**
TQLPPAYTNSFT	22 - 34	Y 28
GVYYPDK	35 - 41	Y 37
GVYYPDK	35 - 41	Y 38
GVYYPDK	35 - 41	Y 37 and Y 38
GVYYPDKVFR	35 - 44	Y 37
GVYYPDKVFR	35 - 44	Y 38
GVYYPDKVFR	35 - 44	Y 37 and Y 38
SWMESEFR	151 - 158	M 153
NIDGYFK	196 - 202	Y 200
SYLTPGDSSSGWTAGAAAYYVGYLQPR	247 - 273	Y 248
SFTVEKGIYQTSNFR	305 - 319	Y 313
GIYQTSNFR	311 - 319	Y 313
FASVYAWNR	347 - 355	Y 351
FASVYAWNR	347 - 355	Y 351 and W 353
ISNCVADYSVLYNSASFSTFK	358 - 378	Y 365
ISNCVADYSVLYNSASFSTFK	358 - 378	Y 369
CYGVSPTK	379 - 386	Y 380
CYGVSPTKLNDLCFTNVYADSFVIRGDEVR	379 - 408	Y 396
LNDLCFTNVYADSFVIR	387 - 403	Y 396

LNDLCFTNVYADSFVIRGDEVR	387 - 408	Y 396 and F 400
IADYNYK	418 - 424	Y 421
IADYNYK	418 - 424	Y 423
VGGNYNYLYR	445 - 454	Y 449
VGGNYNYLYR	445 - 454	Y 451
VGGNYNYLYR	445 - 454	Y 453
VGGNYNYLYR	445 - 454	Y 449 and Y 451
VGGNYNYLYR	445 - 454	Y 451 and Y 453
VYSTGSNVFQTR	635 - 646	Y 636
SFIEDLLFNKVTLADAGFIKQYGDCLGDIAAR	816 - 847	F 833 and Y 837
QYGDCLGDIAAR	836 - 847	Y 837
FNGIGVTQNVLYENQK	906 - 921	Y 917
ASANLAATKMSECVLGQSKR	1020 - 1039	M 1029
ASANLAATKMSECVLGQSK	1020 - 1038	M 1029
MSECVLGQSKRVDFCGK	1029 - 1045	M 1029
MSECVLGQSKR	1029 - 1039	M 1029
MSECVLGQSK	1029 - 1038	M 1029

Fig. 5: Chlorination of tyrosines, phenylalanines and tryptophan and oxidation of methionine of SARS-CoV-2 spike protein by NCT. Spike protein was incubated for 30 min at 37°C in 1% NCT and subjected to mass spectrometry. Positions of chlorinated and oxidized amino acids in the sequence are shown, with 18 tyrosines, two phenylalanines, and one tryptophan chlorinated and two methionines oxidized. No oxidation was found on cysteine.

3C-like proteinase

```
SGFRKMAFPS GKVEGCMVQV TCGTTTLNGL WLDDVVYCPR HVICTSEDML  50
NPNYEDLLIR KSNHNFLVQA GNVQLRVIGH SMQNCVLKLK VDTANPKTPK  100
YKFVRIQPGQ TFSVLACYNG SPSGVYQCAM RPNFTIKGSF LNGSCGSVGF  150
NIDYDCVSFC YMHHMELPTG VHAGTDLEGN FYGPFVDRQT AQAAGTDTTI  200
TVNVLAWLYA AVINGDRWFL NRFTTTLNDF NLVAMKYNYE PLTQDHVDIL  250
GPLSAQTGIA VLDMCASLKE LLQNGMNGRT ILGSALLEDE FTPFDVVRQC  300
SGVTFQ
```

Identified Peptide	Position in Protein	Chlorination Site	Oxidation Site		
			Mono	Di	Tri
KMAFPSGK	5 – 12	-	M6	M6	-
HVICTSEDMLNPNYEDLLIR	41 – 60	Y54	M49	M49, C44	C44
KSNHNFLVQAGNVQLR	61 – 76	H64	-	-	-
VIGHSMQNCVLK	77 – 88	H80	M82	M82, C85	C85
VDTANPKTPKYK	91 – 102	Y101	-	-	-
IQPGQTFSVLACYNGSPSG VYQCAM RPNFTIK	106 – 137	-	M130	-	C117
QTAQAAGTDTTITVNVLA WLYAAVINGDRWFLNR	189 – 222	Y209	-	-	-
FTTTLNDFNLVAMK	223 - 236	-	M235	M235	-
YNYEPLTQDHVDILGPLSAQ TGIAVLDMCASLK	237 – 269	-	M264	-	-
ELLQNGMNGR	270 – 279	-	M276	-	-
QCSGVTFQ	299 – 306	-	-	C300	C300

Fig. 6: Chlorination of tyrosines and histidines and oxidation of methionines and cysteines of SARS-CoV-2 3C-like proteinase by NCT.

Proteinase was incubated for 30 min at 37°C in 1% NCT and subjected to mass spectrometry. Positions of chlorinated and oxidized amino acids in the sequence are shown, with three tyrosines and two histidines chlorinated and seven methionines and four cysteines oxidized.

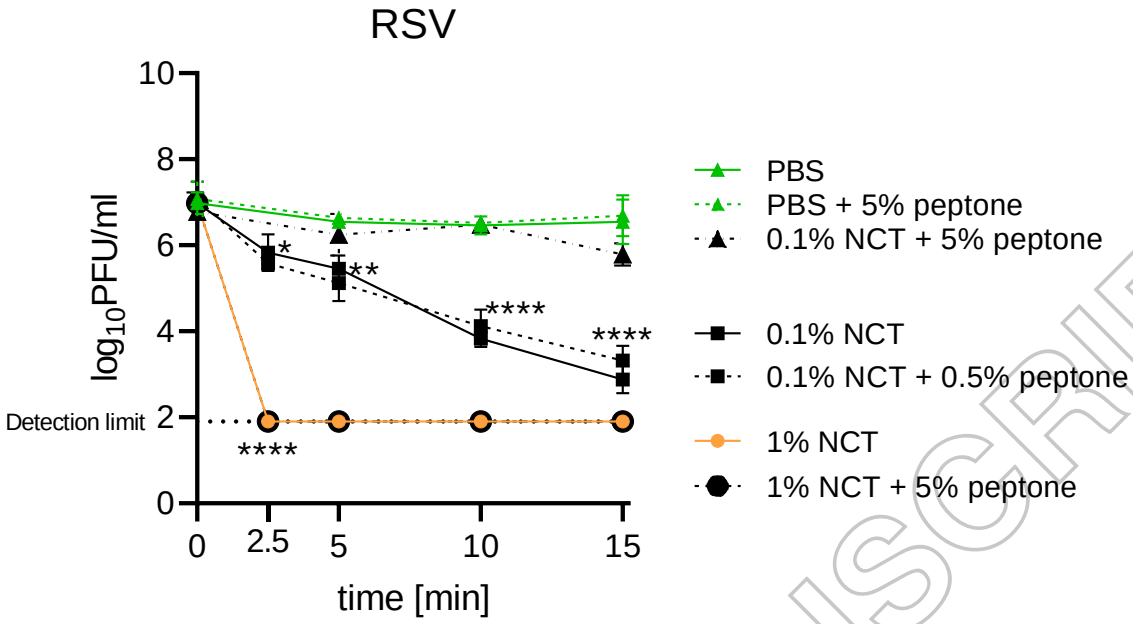

Suppl. Fig. 1: Inactivation of respiratory syncytial virus by NCT in the presence and absence of peptone.

Virus suspension was incubated with 1.0% or 0.1% NCT or PBS in the presence of 5% or 0.5% peptone as indicated for 2.5 min, 5 min, 10 min, and 15 min at 37°C, after which samples were diluted 1:1 in met/his solution for inactivation of NCT. Remaining infectious virus particles were determined using plaque titration. Mean values ± SD of two to four independent experiments. Detection limit 1.90 $\log_{10}$ (dotted line). No difference was found between 0.1% NCT in 5% peptone and the controls and between NCT with and without peptone. * $p < 0.05$, ** $p < 0.01$, *** $p < 0.001$, **** $p < 0.0001$ versus PBS control.

Hemagglutinin

```
MKVKLLILLC TFTATYADTI CIGYHANNST DTVDTVLEKN VTVTHSVNLL  50
EDSHNGKLCL LKGIAPLQLG NCSVAGWILG NPECELLISK ESWSYIVETP  100
NPENGTCYPG YFADYEELRE QLSSVSSFER FEIFPKESSW PNHTVTGVSA  150
SCSHNGKSSF YRNLLWLTGK NGLYPNLSKS YANNKEKEVL VLWGVHHPPN  200
IGDQRALYHT ENAYVSVVSS HYSRRFTPEI AKRPKVRDQE GRINYYWTLL  250
EPGDTIIFEA NGNLIAPRFA FALSRGFGSG IITSNAPMDE CDAKCQTPQG  300
AINSSLPFQN VHPVTIGECP KYVRSTKLRM VTGLRNIPSI QSRGLFGAIA  350
GFIEGGWTGM VDGWYGYHHQ NEQGSGYAAD QKSTQNAING ITNKVNSVIE  400
```

KMNTQFTAVG KEFNKLERRM ENLNKKVDDG FLDIWTYNAE LLVLLENERT 450
LDFHDSNVKN LYEKVKSQLK NNAKEIGNGC FEFYHKCNDE CMESVKNGTY 500
DYPKYSEESK LNREKIDGVK LESMGVYQIL AIYSTVASSL VLLVSLGAIS .550
FWMCSNGSLQ CRICI

Identified Peptide	Position in Protein	Chlorination Site	Oxidation Site		
			Mono	Di	Tri
NLLWLTGK	163 - 170	W166	-	-	-
NGLYPNLSK	171 - 179	Y174	-	-	-
EVLVLWGVHHPPNIGDQR	188 -205	H197	-	-	-
INYYWTLLEPGDTIIFEANGNLIAPR	243 - 268	Y246 or W247	-	-	-
GFGSGIITSNAPMDECDAK	276 - 294	-	M288	-	-
GLFGAIAGFIEGGWTGMVDGWYGYHHQNEQGSGYAADQK	344 - 382	-	M360	-	-
VNSVIEKMNTQFTAVGK	395 - 411	-	M402	-	-
MNTQFTAVGKEFNKLER	402 - 418	-	M402	-	-
MNTQFTAVGKEFNK	402 - 415	-	M402	-	-
MNTQFTAVGK	402 - 411	-	M402	-	-
MENLNKK	420 - 426	-	M420	-	-
MENLNK	420 - 425	-	M420	-	-
TLDFHDSNVK	450 - 459	H454	-	-	-
NGTYDYPK	497 - 504	Y500	-	-	-
NGTYDYPK	497 - 504	Y500, Y502	-	-	-
YSEESKLNR	505 - 513	Y505	-	-	-
YSEESK	505 - 510	Y505	-	-	-

Suppl. Fig. 2: Chlorination of tyrosines, tryptophans, and histidines and oxidation of methionines of hemagglutinin of influenza H1N1 by NCT.

Hemagglutinin was incubated for 30 min at 37°C in 1% NCT and subjected to mass spectrometry. Positions of chlorinated and oxidized amino acids in the sequence

are shown, with four to five tyrosines, one to two tryptophans, and two histidines chlorinated and four methionines oxidized.

Neuraminidase

```
MNPNQKIITI GSVCMTIGMA NLILQIGNII SIWISHSIQL GNQNQIETCN  50
QSVITYENNT WVNQTYVNIS NTNFAAGQSV VSVKLAGNSS LCPVSGWAIY  100
SKDNSVRIGS KGDVFVIREP FISCSPLECR TFFLTQGALL NDKHSNGTIK  150
DRSPYRTLMS CPIGEVPSPY NSRFESVAWS ASACHDGINW LTIGISGPDN  200
GAVAVLKYNG IITDTIKSWR NNILRTQESE CACVNGSCFT VMTDGPSNGQ  250
ASYKIFRIEK GKIVKSVEMN APNYHYEECS CYPDSSEITC VCRDNWHGSN  300
RPWVSFNQNL EYQIGYICSG IFGDNPRPND KTGSCGPVSS NGANGVKGFS  350
FKYGNGVWIG RTKSISSRNG FEMIWDPNGW TGTDNNFSIK QDIVGINEWS  400
GYSGSFVQHP ELTGLDCIRP CFWVELIRGR PKENTIWTSG SSISFCGVNS  450
DTVGWSWPDG AELPFTIDK
```

Identified Peptide	Position in Protein	Chlorination Site	Oxidation Site		
			Mono	Di	Tri
IGSKGDVFVIREPFISCSPLECR	108-130	-	-	C124	-
IGSKGDVFVIREPFISCSPLECR	108-130	-	-	C129	-
IGSKGDVFVIREPFISCSPLECR	108-130	-	-	-	C124
IGSKGDVFVIREPFISCSPLECR	108-130	-	-	-	C129
GDVFVIREPFISCSPLECR	112-130	-	-	C124	-
GDVFVIREPFISCSPLECR	112-130	-	-	C129	-
GDVFVIREPFISCSPLECR	112-130	-	-	-	C124
GDVFVIREPFISCSPLECR	112-130	-	-	-	C129
EPFISCSPLECR	119-130	-	-	C129	-
TLMSCPIGEVPSPYNSR	157-173	-	M159	-	-
TLMSCPIGEVPSPYNSR	157-173	-	-	M159	-
TLMSCPIGEVPSPYNSR	157-173	-	M159	C161	-
TLMSCPIGEVPSPYNSR	157-173	-	M159	-	C161
TLMSCPIGEVPSPYNSR	157-173	Y170	M159	C161	-
TLMSCPIGEVPSPYNSR	157-173	Y170	M159	-	C161
TLMSCPIGEVPSPYNSR	157-173	Y170	M159	-	-
YNGIITDTIKSWR	208-220	Y208	-	-	-
YNGIITDTIK	208-217	Y208	-	-	-

TQESECACVNGSCFTVMTDG PSNGQASYK	226-254	-	M242	-	-
TGSCGPVSSNGANGVK	332-347	-	-	C335	-
TGSCGPVSSNGANGVK	332-347	-	-	-	C335
YGNGVWIGR	353-361	Y353	-	-	-

Suppl. Fig. 3: Chlorination of tyrosines and oxidation of methionines and cysteines of neuraminidase of influenza H1N1 by NCT.

Neuraminidase was incubated for 30 min at 37°C in 1% NCT and subjected to mass spectrometry. Positions of chlorinated and oxidized amino acids in the sequence are shown, with three tyrosines chlorinated and two methionines and four cysteines oxidized.

Fusion Glycoprotein

```
MELPILKTNA ITAILAAVTL CFASSQNITE EFYQSTCSAV SKGYLSALRT  50
GWYTSVITIE LSNIKENKCN GTDAKVKLIK QELDKYKSAV TELQLLMQST  100
PATNNRARRE LPRFMNYTLN NTKNTNVTLS KKRKRRFLGF LLGVGSAIAS  150
GIAVSKVLHL EGEVNKIKSA LLSTNKAVVS LSNGVSVLTS KVLDLKNYID  200
KQLLPIVNKQ SCSISNIETV IEFQQKNNRL LEITREFSVN AGVTTPVSTY  250
MLTNSELLSL INDMPITNDQ KKLMSNNVQI VRQQSYSIMS IIKEEVLAYV  300
VQLPLYGVID TPCWKLHTSP LCTTNTKEGS NICLTRTDRG WYCDNAGSVS  350
FFPLAETCKV QSNRVFCDTM NSLTLPSEVN LCNIDIFNPK YDCKIMTSKT  400
DVSSSVITSL GAIVSCYGKT KCTASNKDRG IIKTFSNGCD YVSNKGVDTV  450
SVGNTLYYVN KQEGKSLYVK GEPIINFYDP LVFPSDEFDA SISQVNEKIN  500
QSLAFIRKSD ELLHNVNAGK STTNIMITTI IIVIIVILLS LIAVGLLLYC  550
KARSTPVTLS KDQLSGINNI AFS
```

Identified Peptide	Position in Protein	Chlorination Site	Oxidation Site		
			Mono	Di	Tri
GYLSALR	43-49	Y44	-	-	-
LIKQELDKYK	78-87	Y86	-	-	-
QELDKYK	81-87	Y86	-	-	-
FMNYTLNNTK	114-123	-	M115	-	-
VLDLKNYIDK	192-201	Y198	-	-	-
NYIDKQLLPIVNK	197-209	Y198	-	-	-

EFSVNAGVTTPVSTYMLTNSELLSLINDMPITNDQKK	236-272	-	M264	-	-
EFSVNAGVTTPVSTYMLTNSELLSLINDMPITNDQKK	236-272	-	M251, M264	-	-
KLMSNNVQIVR	272-282	-	M274	-	-
KLMSNNVQIVR	272-282	-	-	M274	-
LMSNNVQIVR	273-282	-	M274	-	-
LMSNNVQIVR	273-282	-	-	M274	-
QQSYSIMSIIK	283-293	-	M289	-	-
QQSYSIMSIIK	283-293	Y286	-	-	-
LHTSPLCTTNTKEGSNICLTR	316-336	-	C333	-	-
LHTSPLCTTNTK	316-327	-	C322	-	-
LHTSPLCTTNTK	316-327	-	-	C322	-
LHTSPLCTTNTK	316-327	-	--	-	C322
EGSNICLTR	328-336	-	-	-	C333
YDCKIMTSKTDVSSSVITSLGAIVSCYGK	391-419	-	M396	-	-
YDCKIMTSK	391-399	-	M396	-	-
YDCKIMTSK	391-399	Y391	M396	-	-
IMTSKTDVSSSVITSLGAIVSCYGKTK	395-421	-	M396	-	-
IMTSKTDVSSSVITSLGAIVSCYGK	395-419	-	M396	-	-
IMTSKTDVSSSVITSLGAIVSCYGK	395-419	Y417	M396	-	-
GVDTVSVGNTLYYVNKQEGK	446-465	Y457 or Y458	-	-	-

Suppl. Fig. 4: Chlorination of tyrosines and oxidation of methionines and cysteines of fusion glycoprotein of RSV by NCT. Fusion glycoprotein was incubated for 30 min at 37°C in 1% NCT and subjected to mass spectrometry. Positions of chlorinated and oxidized amino acids in the sequence are shown, with seven tyrosines chlorinated and six methionines and two cysteines oxidized.